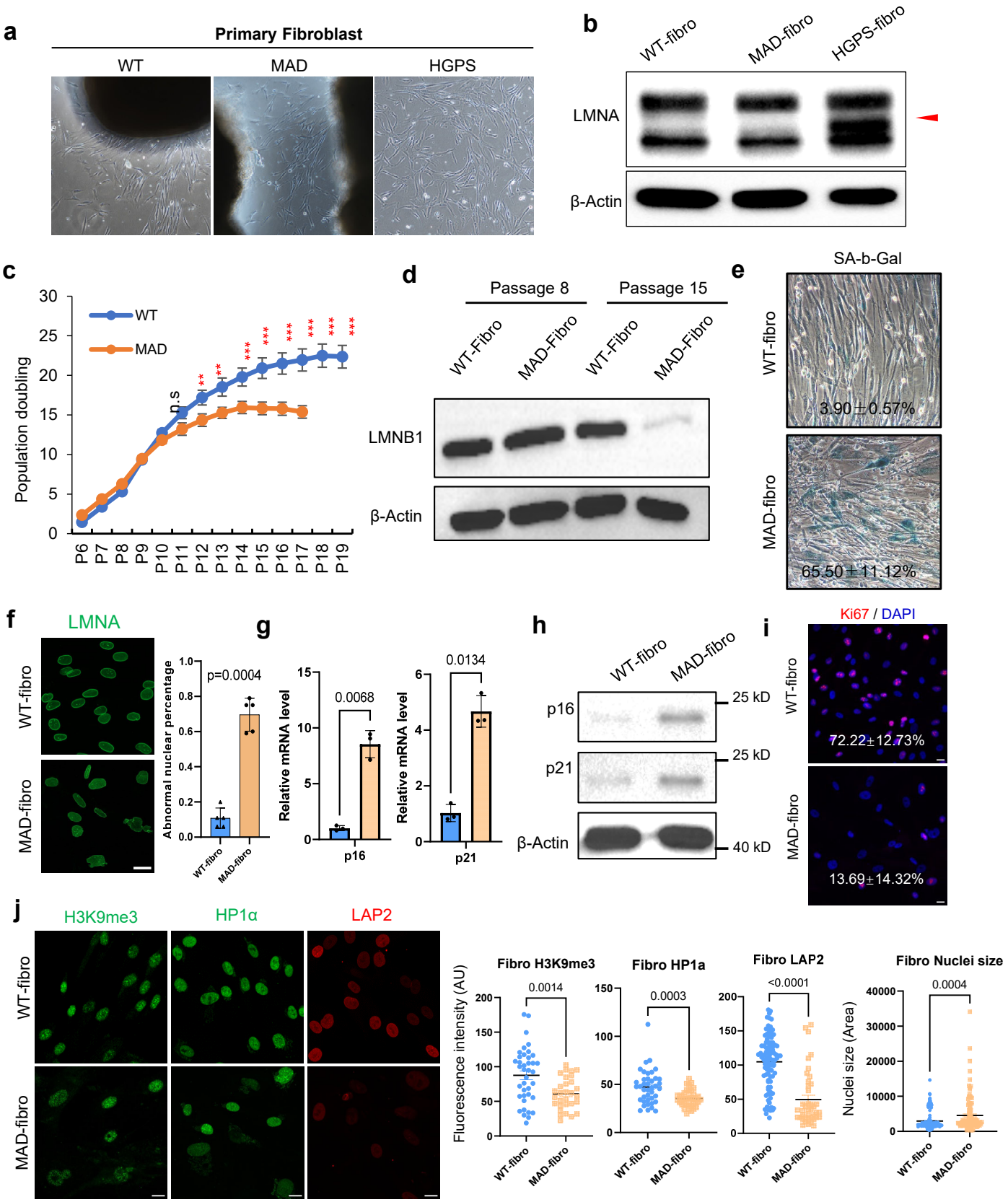
a
Primary Fibroblast
WT
MAD
HGPS
b
WT-fibro
MAD-fibro
HGPS-fibro
LMNA
β-Actin
c
Population doubling
WT
MAD
n.s
**
***
P6
P7
P8
P9
P10
P11
P12
P13
P14
P15
P16
P17
P18
P19
d
Passage 8
Passage 15
WT-Fibro
MAD-Fibro
LMNB1
β-Actin
e
SA-b-Gal
WT-fibro
MAD-fibro
3.90±0.57%
65.50±11.12%
f
LMNA
WT-fibro
MAD-fibro
Abnormal nuclear percentage
p=0.0004
g
Relative mRNA level
0.0068
p16
0.0134
p21
h
WT-fibro
MAD-fibro
p16
p21
β-Actin
25 kD
25 kD
40 kD
i
Ki67 / DAPI
WT-fibro
MAD-fibro
72.22±12.73%
13.69±14.32%
j
H3K9me3
HP1α
LAP2
WT-fibro
MAD-fibro
Fluorescence intensity (AU)
Fibro H3K9me3
0.0014
Fibro HP1a
0.0003
Fibro LAP2
<0.0001
Fibro Nuclei size
Nuclei size (Area)
0.0004

Supplementary Fig. 1| MAD patient-derived fibroblasts exhibited premature senescence. a, Isolation of primary fibroblasts from normal, MAD and HGPS patients. The normal fibroblasts were labeled as WT. b, Immunoblotting of lamin A/C in primary fibroblasts from normal individual, MAD and HGPS patients. The red arrow indicated progerin. β-Actin served as the loading control. The results were repeated twice with similar results. c, Growth curve of MAD primary fibroblasts. Bars represent the mean ± SD.; n = 3 independent biological replicates; **p < 0.01, ***p < 0.001; n.s., non-significant; p value was calculated using two-way ANOVA test. d, Immunoblotting of lamin B1 in MAD primary fibroblasts during different passages (early passage p8 and late passage p15). The results were repeated twice with similar results. e, SA-β-gal staining passage 15 of MAD primary fibroblasts, the labeled number indicates positive percentage; Scale bar 100 μm. Data are mean ± SD, the p value was calculated using two-tailed unpaired t-test, n = 3. Three biological replicates were performed with similar results. f, Immunostaining of lamin A/C (LMNA, green) in WT and MAD fibroblasts. DAPI, blue. Scale bar 10 μm. Data represent the mean ± SD, the p value was calculated using two-tailed unpaired t-test, n=5. Three biological replicates were performed with similar results. g, qPCR analysis of *p16* and *p21* using late passage fibroblasts. Data were normalized to *18S rDNA* and represent mean ± SD, n=3 independent biological replicates; p values were calculated using a one-way analysis of variance (ANOVA). h, Immunoblotting of p16 and p21 using late passage fibroblasts. The results were repeated twice with similar results. i, Representative images of Ki67 staining (red) in WT and MAD-fibroblast. DAPI, blue. Scale bar 10 μm. Data indicates the mean ± SD, the p value was calculated using two-tailed unpaired t-test, n=3. Images were acquired from three independent biological replicates with similar results. j, Representative images of heterochromatin associated HP1a (green, n=40 WT and n=38 MAD), H3K9me3 (green, n=39 WT and n=30 MAD), LAP2 (red, n=99 WT and n=41 MAD) and nuclei size (n=178 WT and n=109 MAD). Scale bars 10 μm. Images were acquired from three independent biological replicates with similar results. Fluorescence intensity was quantified and p values were calculated by unpaired two-tailed Student's t-test. Source data are provided as a Source Data file.

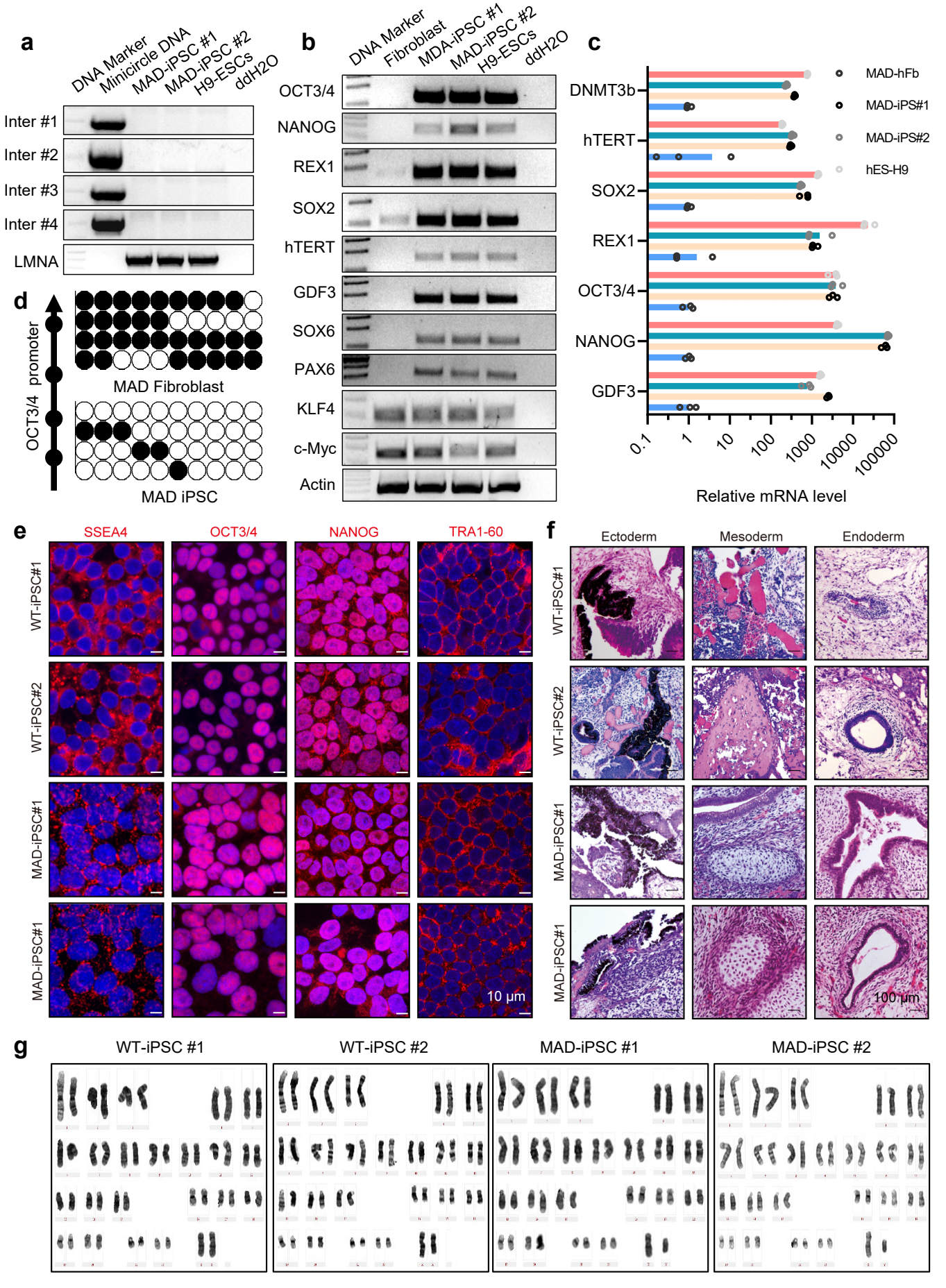
a
DNA Marker
Minicircle DNA
MAD-iPSC #1
MAD-iPSC #2
H9-ESCs
ddH2O
Inter #1
Inter #2
Inter #3
Inter #4
LMNA
b
DNA Marker
Fibroblast
MDA-iPSC #1
MAD-iPSC #2
H9-ESCs
ddH2O
OCT3/4
NANOG
REX1
SOX2
hTERT
GDF3
SOX6
PAX6
KLF4
c-Myc
Actin
c
MAD-hFb
MAD-iPS#1
MAD-iPS#2
hES-H9
DNMT3b
hTERT
SOX2
REX1
OCT3/4
NANOG
GDF3
0.1
1
10
100
1000
10000
100000
Relative mRNA level
d
OCT3/4 promoter
MAD Fibroblast
MAD iPSC
e
SSEA4
OCT3/4
NANOG
TRA1-60
WT-iPSC#1
WT-iPSC#2
MAD-iPSC#1
MAD-iPSC#1
10 μm
f
Ectoderm
Mesoderm
Endoderm
WT-iPSC#1
WT-iPSC#2
MAD-iPSC#1
MAD-iPSC#1
100 μm
g
WT-iPSC #1
WT-iPSC #2
MAD-iPSC #1
MAD-iPSC #2

Supplementary Fig. 2| Generation of induced pluripotent stem cells (iPSCs) from MAD fibroblasts via integration-free minicircle vector. a, Examination of vector integration in WT and MAD-iPSCs clones with 4 pairs of primers flanking different regions. Minicircle DNA served as a positive control while H9-ESCs as a negative control. b, RT-PCR of pluripotency related genes in MAD iPSC and fibroblast cells. c, qPCR of pluripotency related genes in MAD-iPSCs and parental fibroblasts. H9 served as a positive control. Data were normalized to *GAPDH* and represent mean ± SD, n=3 independent biological replicates. Three independent biological replicates were performed with similar results. d, Bisulfite sequencing of OCT3/4 promoter region in MAD fibroblasts and MAD-iPSCs#1. Blank and filled circle represent unmethylated and methylated CpGs, respectively. Each row of circles represents sequence result from a given amplicon and ten amplicons were sequenced and analyzed. e, Immunostaining of pluripotency associated markers in MAD-iPSCs, including SSEA-4 (red), NANOG (red), OCT3/4 (red) and TRA60-1 (red) in WT- and MAD-iPSCs. DAPI, blue. Scale bar 10 μm. Three independent biological replicates were performed with similar results. f, Examination of three germ layers differentiation capability of WT- and MAD-iPSCs. Scale bar 100 μm. Three biological replicates were performed with similar results. g, Representative M-phase karyotyping in WT- and MAD-iPSCs clones. Source data are provided as a Source Data file.

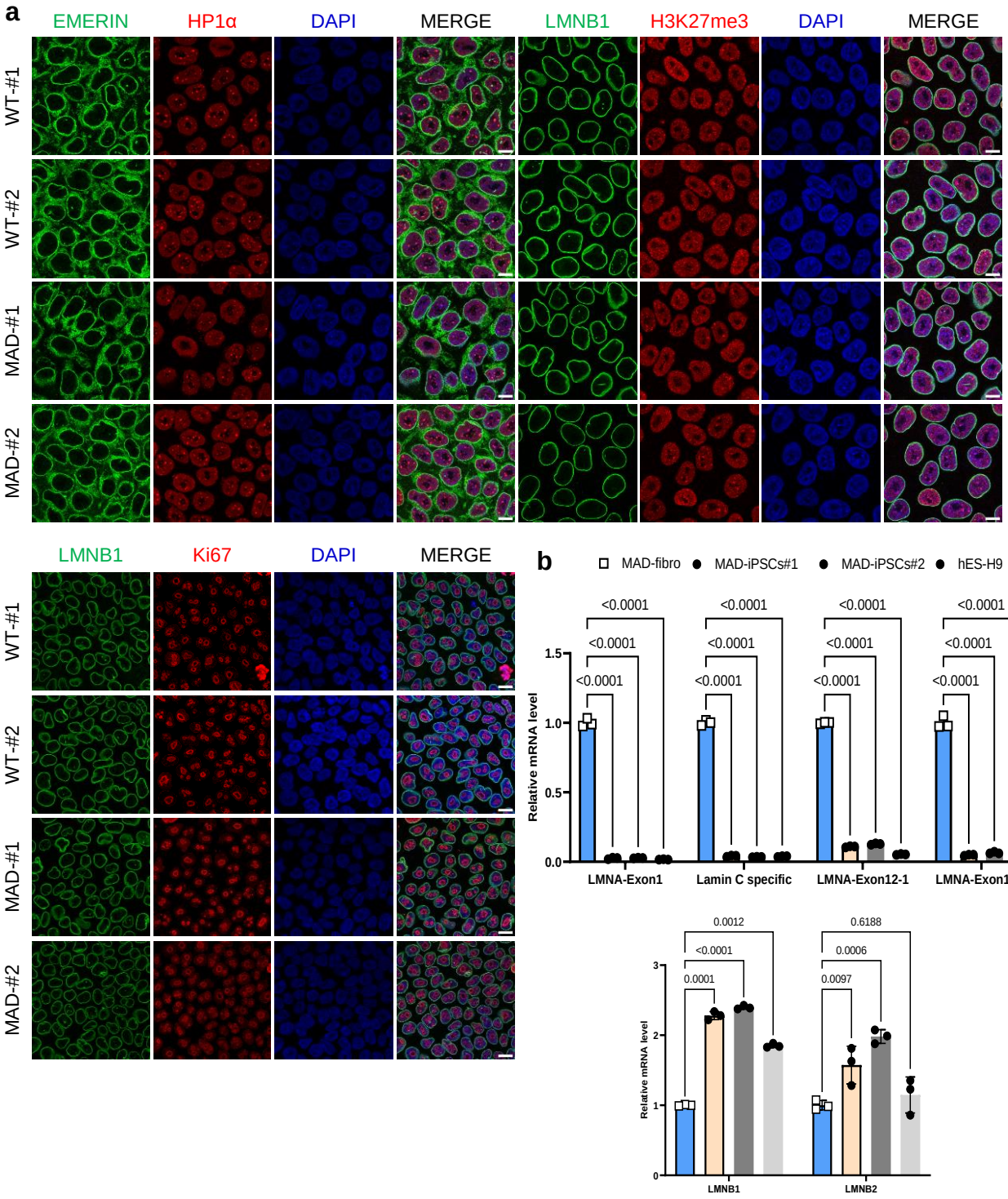
a
EMERIN
HP1α
DAPI
MERGE
LMNB1
H3K27me3
DAPI
MERGE
WT-#1
WT-#2
MAD-#1
MAD-#2
LMNB1
Ki67
DAPI
MERGE
WT-#1
WT-#2
MAD-#1
MAD-#2
b
MAD-fibro
MAD-iPSCs#1
MAD-iPSCs#2
hES-H9
Relative mRNA level
<0.0001
LMNA-Exon1
Lamin C specific
LMNA-Exon12-1
LMNA-Exon12-2
0.0012
0.0001
0.6188
0.0006
0.0097
LMNB1
LMNB2

Supplementary Fig. 3| Characterization of MAD-iPSCs. a, Immunostaining of HP1a (red), EMERIN (green), lamin B1 (LMNB1, green) and H3K27me3 (red), lamin B1 (LMNB1, green) and Ki-67 (red) in iPSCs clones. DAPI, blue. Scale bar 10 μm. Three independent biological replicates were performed with similar results. b, qPCR analysis of *LMNB1*, *LMNB2*, *Lamin A* and *Lamin C* in MAD-iPSCs. Gene expression levels were normalized to *GAPDH* and relative expressions of genes were plotted against that in fibroblasts. H9-ESCs served as control. Data represent mean ± SD, n=3 independent samples; p values were calculated using one-way ANOVA coupled with Tukey's post hoc test. Three independent biological replicates were performed with similar results. Source data are provided as a Source Data file.

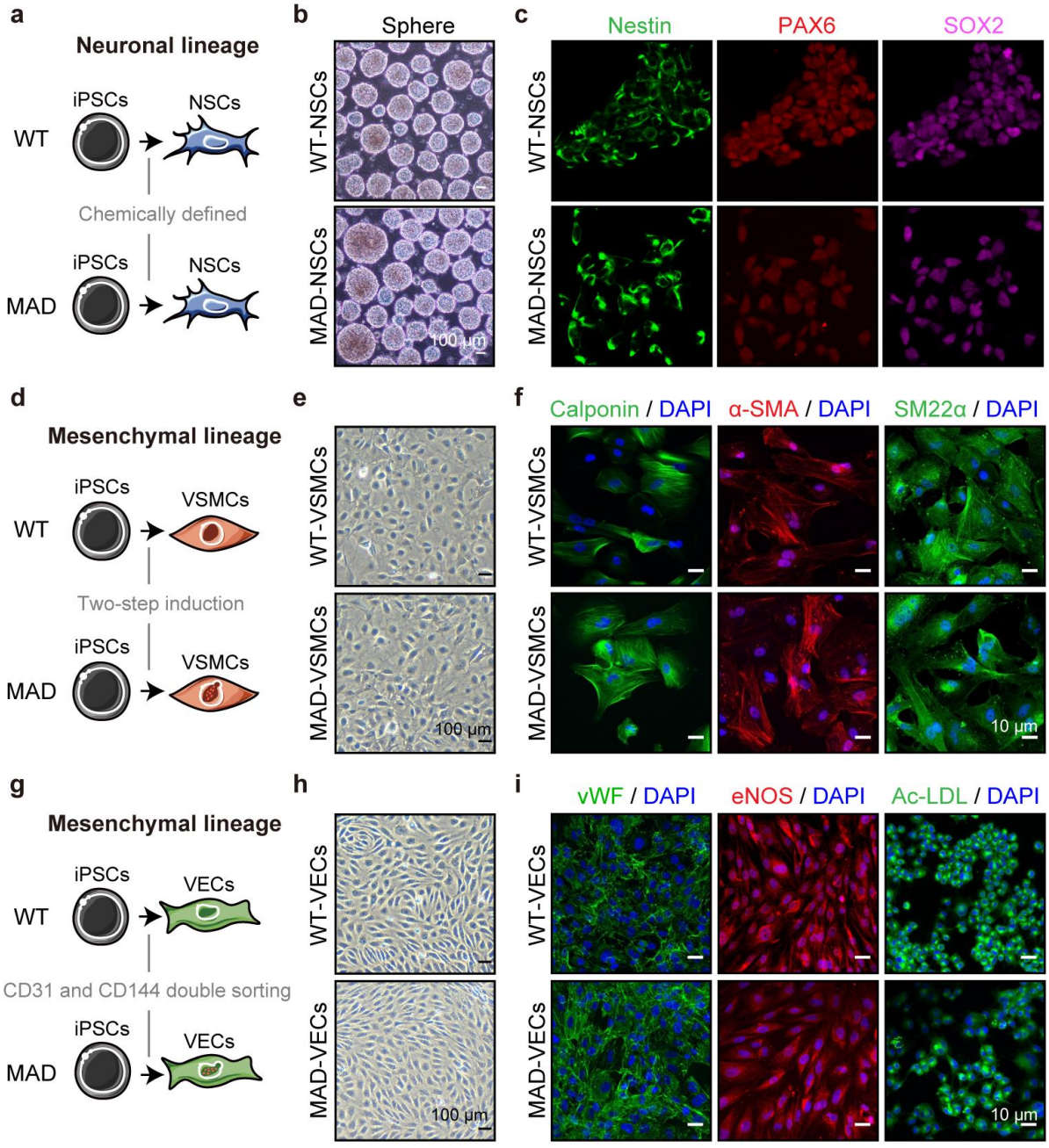
a
Neuronal lineage
iPSCs
NSCs
WT
Chemically defined
iPSCs
NSCs
MAD
b
Sphere
WT-NSCs
MAD-NSCs
100 μm
c
Nestin
PAX6
SOX2
WT-NSCs
MAD-NSCs
d
Mesenchymal lineage
iPSCs
VSMCs
WT
Two-step induction
iPSCs
VSMCs
MAD
e
WT-VSMCs
MAD-VSMCs
100 μm
f
Calponin / DAPI
α-SMA / DAPI
SM22α / DAPI
WT-VSMCs
MAD-VSMCs
10 μm
g
Mesenchymal lineage
iPSCs
VECs
WT
CD31 and CD144 double sorting
iPSCs
VECs
MAD
h
WT-VECs
MAD-VECs
100 μm
i
vWF / DAPI
eNOS / DAPI
Ac-LDL / DAPI
WT-VECs
MAD-VECs
10 μm

j

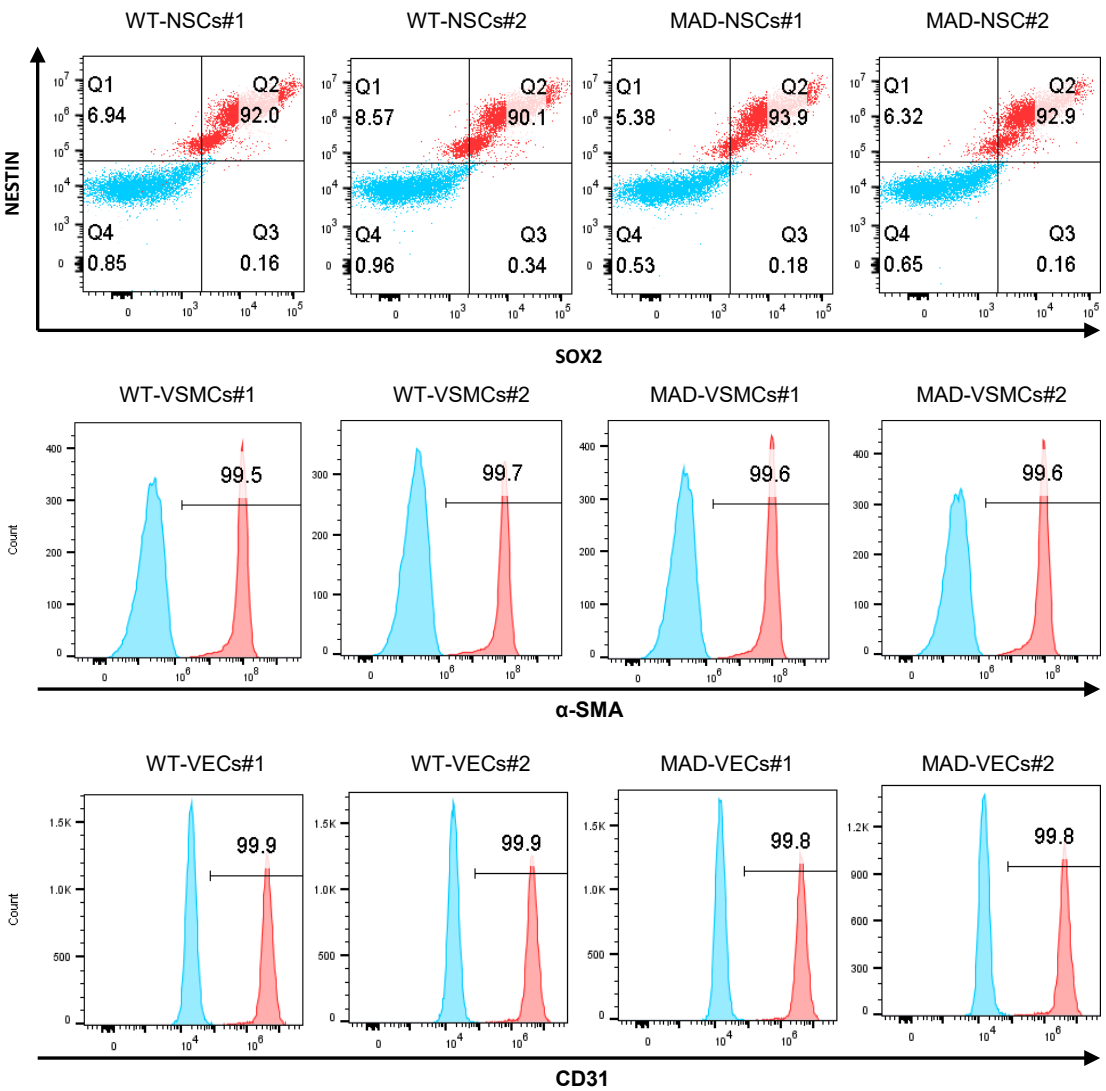
WT-NSCs#1
WT-NSCs#2
MAD-NSCs#1
MAD-NSC#2
NESTIN
Q1
Q2
Q3
Q4
6.94
92.0
0.85
0.16
8.57
90.1
0.96
0.34
5.38
93.9
0.53
0.18
6.32
92.9
0.65
0.16
SOX2
WT-VSMCs#1
WT-VSMCs#2
MAD-VSMCs#1
MAD-VSMCs#2
Count
99.5
99.7
99.6
99.6
α-SMA
WT-VECs#1
WT-VECs#2
MAD-VECs#1
MAD-VECs#2
Count
99.9
99.9
99.8
99.8
CD31

Supplementary Fig. 4| Characterization of NSCs, VSMCs and VECs derived from MAD-iPSCs. a, Schematic diagram of NSCs induction from iPSCs. b, Neural-spheres derived from WT-iPSCs and MAD-iPSCs. Scale bar 100 μm. c, Co-immunostaining of NSCs specific markers, including NESTIN (green), PAX6 (red), SOX2 (pink) at passage 6. Scale bar 10 μm. Three independent differentiations were performed with similar results. d, Schematic diagram of VSMCs from iPSCs. e. VSMCs derived from WT- and MAD-iPSCs. Scale bars, 100 μm. f, Immunostaining of VSMCs specific markers, including Calponin (Green), α-SMA (red), SM22 α (green) at passage 5. DAPI, blue. Scale bar 10μm. Three independent differentiations were performed with similar results. g-i, Schematic diagram of VECs induction from iPSCs. h, VECs derived from WT- and MAD-iPSCs with double selections of CD31/CD144. Scale bars, 100 μm. i, Immunostaining of specific markers, including vWF (green), eNOS (red) and functional assay (Ac-LDL) of VECs derived from WT and MAD-iPSCs at passage 3. DAPI, blue. Scale bars, 10 μm. Three independent biological differentiation were performed with similar results. j, Flow cytometry analysis of two iPSCs clone derived NSCs, VSMCs and VECs with corresponding antibodies (NESTIN and SOX2 for NSCs, α-SMA for VSMCs and CD31 for VECs). Three independent differentiations were performed with similar results.

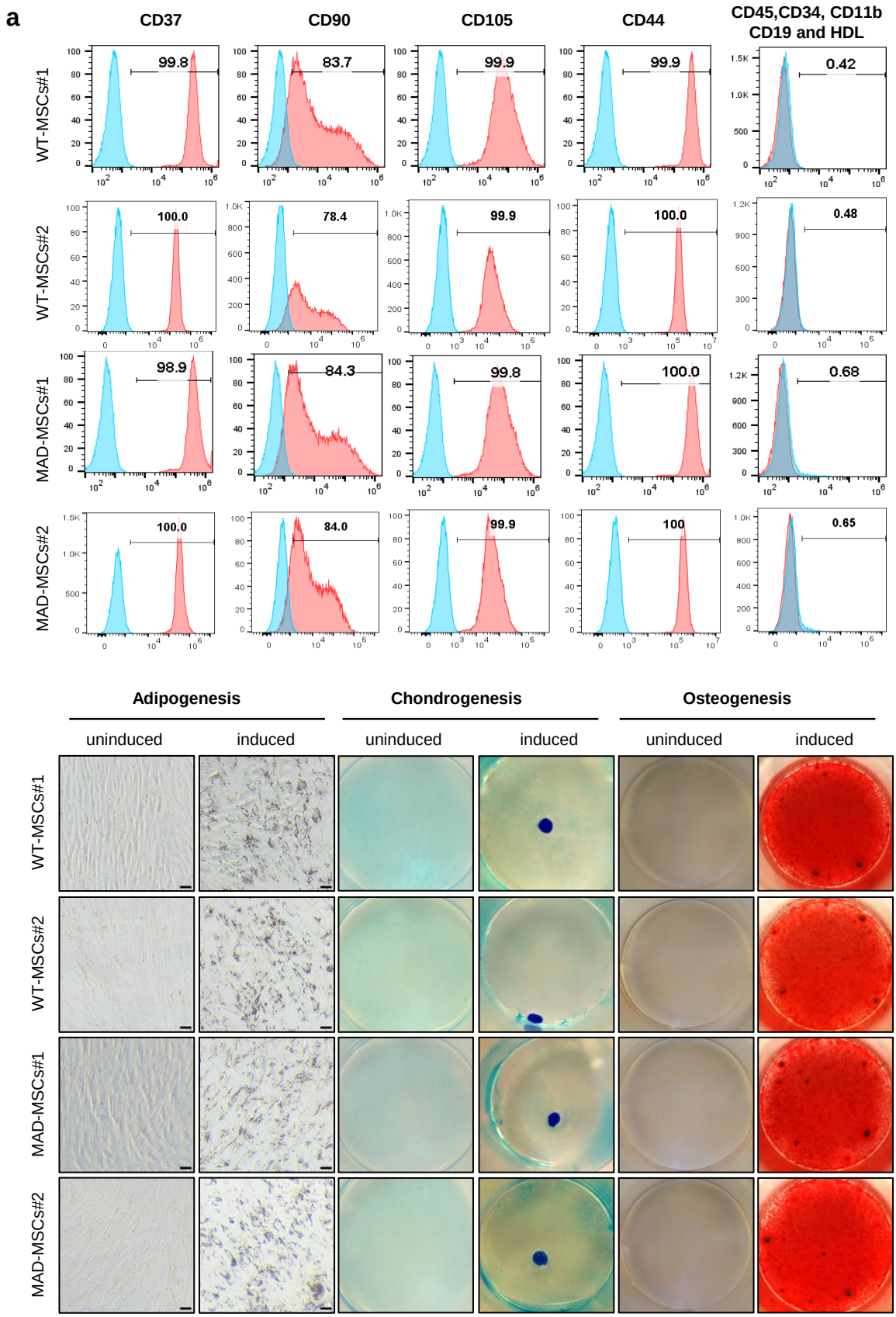
a
CD37
CD90
CD105
CD44
CD45,CD34, CD11b
CD19 and HDL
WT-MSCs#1
WT-MSCs#2
MAD-MSCs#1
MAD-MSCs#2
99.8
83.7
99.9
99.9
0.42
100.0
78.4
99.9
100.0
0.48
98.9
84.3
99.8
100.0
0.68
100.0
84.0
99.9
100
0.65
b
Adipogenesis
Chondrogenesis
Osteogenesis
uninduced
induced
uninduced
induced
uninduced
induced
WT-MSCs#1
WT-MSCs#2
MAD-MSCs#1
MAD-MSCs#2

Supplementary Fig. 5| MAD-iPSCs derived mesenchymal stem cells (MAD-MSCs) recapitulate accelerated aging. a, Flow cytometry analyses of the surface markers in MSCs (P5 MSCs) derived from two iPSCs clones. Three independent differentiations were performed with similar results. b, iPSCs clones derived MSCS for trilineage differentiation. Adipogenesis, osteogenesis and chondrogenesis in WT- and MAD-MSCs (P5 MSCs) were examined by Oil red (Scale bars 200 μm), Alizarin red (Scale bars are 100 μm) and Alcian blue (Scale bars are 200 μm) staining. Three independent biological replicates were performed with similar results.

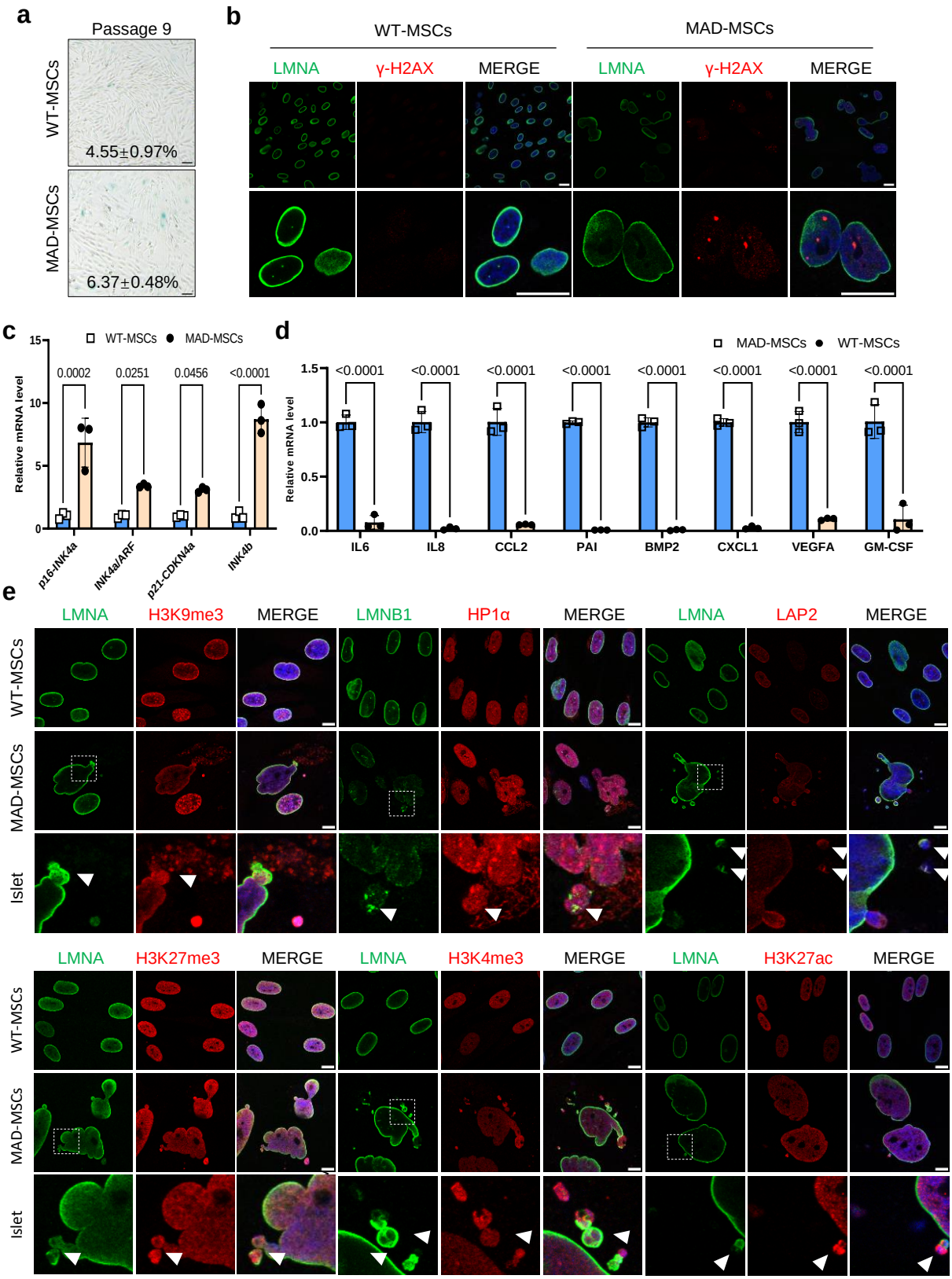
a
Passage 9
WT-MSCs
MAD-MSCs
4.55±0.97%
6.37±0.48%
b
WT-MSCs
MAD-MSCs
LMNA
γ-H2AX
MERGE
c
WT-MSCs
MAD-MSCs
Relative mRNA level
0.0002
0.0251
0.0456
<0.0001
p16-INK4a
INK4a/ARF
p21-CDKN4a
INK4b
d
MAD-MSCs
WT-MSCs
Relative mRNA level
<0.0001
IL6
IL8
CCL2
PAI
BMP2
CXCL1
VEGFA
GM-CSF
e
LMNA
H3K9me3
MERGE
LMNB1
HP1α
LAP2
WT-MSCs
MAD-MSCs
Islet
H3K27me3
H3K4me3
H3K27ac

f

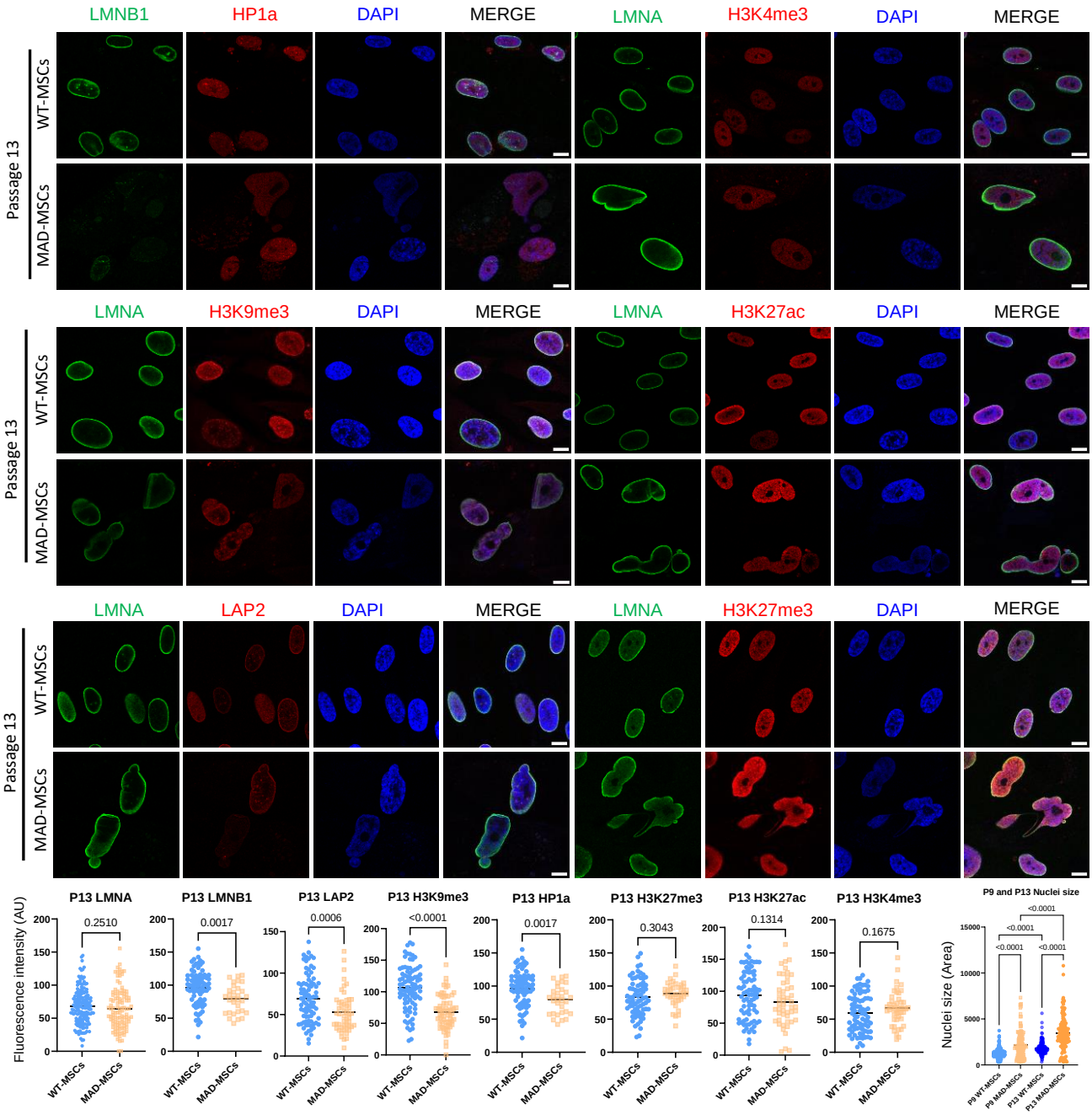
LMNB1
HP1a
DAPI
MERGE
LMNA
H3K4me3
DAPI
MERGE
Passage 13
WT-MSCs
MAD-MSCs
LMNA
H3K9me3
DAPI
MERGE
LMNA
H3K27ac
DAPI
MERGE
LMNA
LAP2
DAPI
MERGE
LMNA
H3K27me3
DAPI
MERGE
Fluorescence intensity (AU)
P13 LMNA
0.2510
P13 LMNB1
0.0017
P13 LAP2
0.0006
P13 H3K9me3
<0.0001
P13 HP1a
0.0017
P13 H3K27me3
0.3043
P13 H3K27ac
0.1314
P13 H3K4me3
0.1675
WT-MSCs
MAD-MSCs
P9 and P13 Nuclei size
Nuclei size (Area)
<0.0001
P9 WT-MSCs
P9 MAD-MSCs
P13 WT-MSCs
P13 MAD-MSCs

Supplementary Fig. 6| MAD-MSCs exhibited accelerated exhaustion. a, SA-β-gal staining of early passage (passage 9) of MAD-MSCs, the labeled number indicates positive percentage. Data are mean ± SD, the p value was calculated using two-tailed unpaired t-test, n = 3. Three independent biological replicates were performed with similar results. b, Immunostaining of lamin A/C (LMNA, green) and γ-H2A.X (red). DAPI, blue. Scale bar 10 μm. c-d, qPCR of the cell cycle arrest genes and inflammasome associated genes. Data were normalized to *18S rDNA* and represent mean ± SD; n=3 independent samples, p values were calculated with one-way ANOVA coupled with Tukey's post hoc test. e, Immunostaining of nuclear lamin and histone markers shows nuclear budding, including active and repressive markers. Scale bars, 10 μm. f, Immunostaining and quantification of nuclear lamin and histone markers in passage 13 MSCs. Lamin B1 and HP1a (WT n=77, MAD n=31), lamin A/C (WT n=168, MAD n=92), LAP2 (WT n=80, MAD n=28), H3K9me3 (WT n=88, MAD n= 64), H3K27me3 (WT n=181, MAD n= 41), H3K27ac (WT n=80, MAD n= 49), H3K4me3 (WT n=138, MAD n= 52) and nuclei size (WT n=155, MAD n= 137). Data are mean ± SD; the lines in scatter dot plot indicate the averaged intensity and the p values were calculated using two-tailed unpaired t-test. The images were repeated from three independent biological experiments with similar results. Source data are provided as a Source Data file.

a

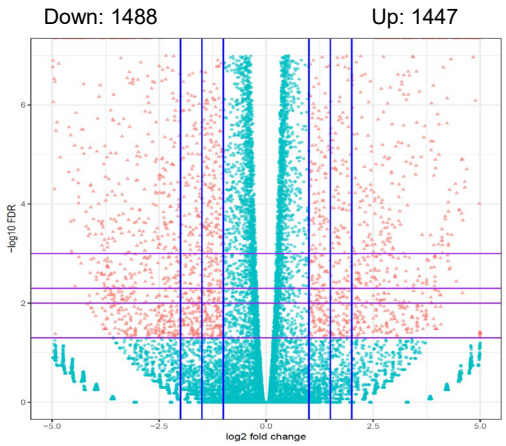

b

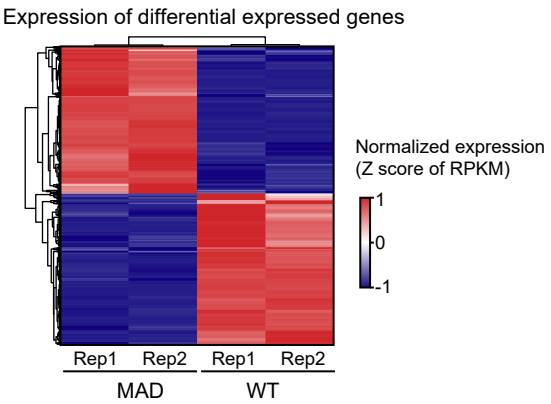

c

GAD DISEASE	# GENE	p value
Blood Pressure	97	6.90E-11
Heart Failure	80	6.40E-09
Myocardial Infarction	100	2.50E-08
Autism	74	2.80E-08
Echocardiography	77	7.80E-08
Heart Rate	57	3.80E-07
Glucose	51	2.80E-06
Cardiomyopathy	16	1.50E-05
Stroke	90	2.10E-05
Body Weight	70	8.10E-05
Body Height	91	8.80E-05
Bone Mineral Density	69	1.50E-04
Bone Density	42	3.50E-04
Hypertension	103	7.80E-04
Obesity	60	9.80E-04
Dilated cardiomyopathy	12	2.40E-03
Arteries	30	2.70E-03
Hyperparathyroidism, Secondary	28	3.10E-03
Dementia, Vascular	6	3.70E-03
kidney aging	20	8.00E-03
Fibrinogen	27	8.00E-03
Myocardial infarct	23	8.70E-03
Osteoarthritis	15	8.90E-03
Atherosclerosis	53	1.10E-02
Blood Coagulation Factor Inhibitors	4	3.10E-02
Heart disease, ischemic	10	3.50E-02

d

GAD DISEASE	# GENE	p value
Bone Mineral Density	61	3.10E-06
Pharmacogenetic studies	23	3.00E-05
Atherosclerosis	48	3.80E-04
Hypertension	81	7.60E-04
Endometriosis	19	8.50E-04
Weight loss	8	8.60E-04
Type 2 Diabetes	213	1.00E-03
Nasopharyngeal Neoplasms	11	1.10E-03
Lymphoma, Non-Hodgkin	35	1.40E-03
Brain Ischemia|Stroke	18	1.40E-03
Premature ovarian failure	35	1.50E-03
1-hydroxypyrene, urinary	6	1.60E-03
Birth Weight|Body Weight	4	1.90E-03
left ventricular hypertrophy	9	1.90E-03
Diabetes, type 1	28	2.30E-03
Myocardial Infarction	62	2.90E-03
Pulmonary Disease	16	3.40E-03
Multiple myeloma	22	4.20E-03
Chronic renal failure|Kidney Failure	95	4.40E-03
Hypertension; blood pressure	4	4.50E-03
Pregnancy loss, recurrent	12	4.80E-03
Aging	9	5.40E-03
Chronic obstructive pulmonary disease	49	5.40E-03
Vascular Diseases	5	5.70E-03
Atherosclerosis, coronary	23	5.70E-03
Macular Degeneration	7	6.20E-03

e

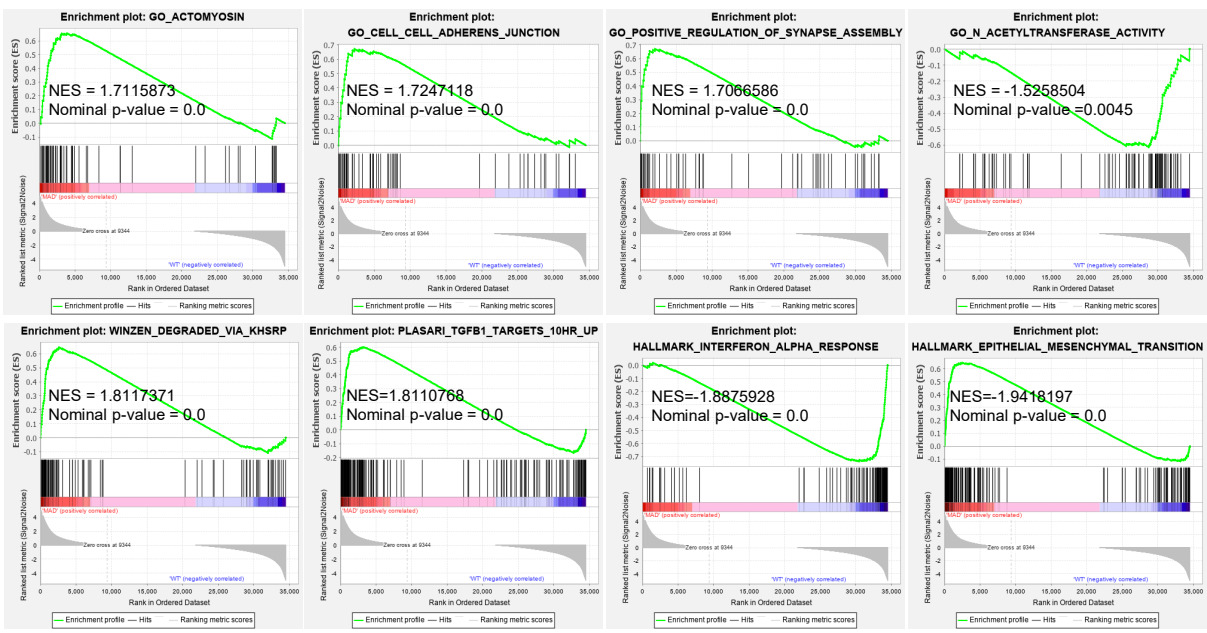

Supplementary Fig. 7| Transcriptome analysis of MAD-MSCs. a-b, Volcano plot and heatmap of differentially expressed genes in WT-MSCs and MAD-MSCs based on RNA sequencing (two replicated of each sample, FDR<0.05). The number of upregulated and downregulated genes are indicated. c-d, Diseases enrichment of differentially expressed genes in MAD-MSCs according to GAD database, upregulated enrichment (c) and downregulated enrichment (d). Enriched gene number and p value were indicated. e, Representative GSEA enriched pathways, enrichment score and p value were indicated. All p-values were determined using the two-sided Wilcoxon rank-sum test.

a **Senecence of hMSCs**

Symbol	Ref	Senecence	Symbol	Ref	Senecence
WS_hMPC	Wang, 2021, *Sci Tranl Med*	Accelerated	CLOCK_KO	Liang, 2019, *Cell Res*	Accelerated
SenecenceDriver	Wang, 2021, *Sci Tranl Med*	Accelerated	RAP1_KO	Zhang, 2018, *Protein Cell*	Alleviated
WS_hMSC	Shan, 2021, *Protein Cell*	Accelerated	CBX4_KO	Ren, 2019, *Cell Rep*	Accelerated
HGPS_hMSC	Shan, 2021, *Protein Cell*	Accelerated	ATF6_KO	Wang, 2018, *Cell Discov*	Accelerated
GAtreatWS	Shan, 2021, *Protein Cell*	Alleviated	SIRT6_KO	Pan, 2016, *Cell Res*	Accelerated
GAtreatHGPS	Shan, 2021, *Protein Cell*	Alleviated	NRF2_mut	Yang, 2017 *Cell Res*	Alleviated
SIRT7_KO	Bi, 2020, *Protein Cell*	Accelerated	WRN_KO	Zhang, 2015, *Science*	Accelerated
SIRT3_KO	Diao, 2021, *Nucleic Acids Res*	Accelerated	Irradiation	Sepúlveda, 2014, *Stem Cells*	Accelerated
ZKSCAN3_KO	Hu, 2021, *Nucleic Acids Res*	Accelerated	TERT_OE	Estrada, 2013, *Cell Death Dis*	Alleviated
FOXD1_KO	Fu, 2019, *Plos Bio*	Accelerated	NormalSenecent	Benisch, 2012, *Plos One*	Accelerated
YAP_KO	Fu, 2019, *Plos Bio*	Accelerated	AgeCorrelate	Alves, 2012, *Plos One*	Accelerated
DGCR8_mut	Deng, 2019, *Nat Commun*	Accelerated	NormalOld	Benisch, 2012, *Plos One*	Accelerated
FOXO3_mut	Yan, 2019, *Cell Stem Cell*	Alleviated	HGPS	Zhang, 2011, *Cell Stem Cell*	Accelerated

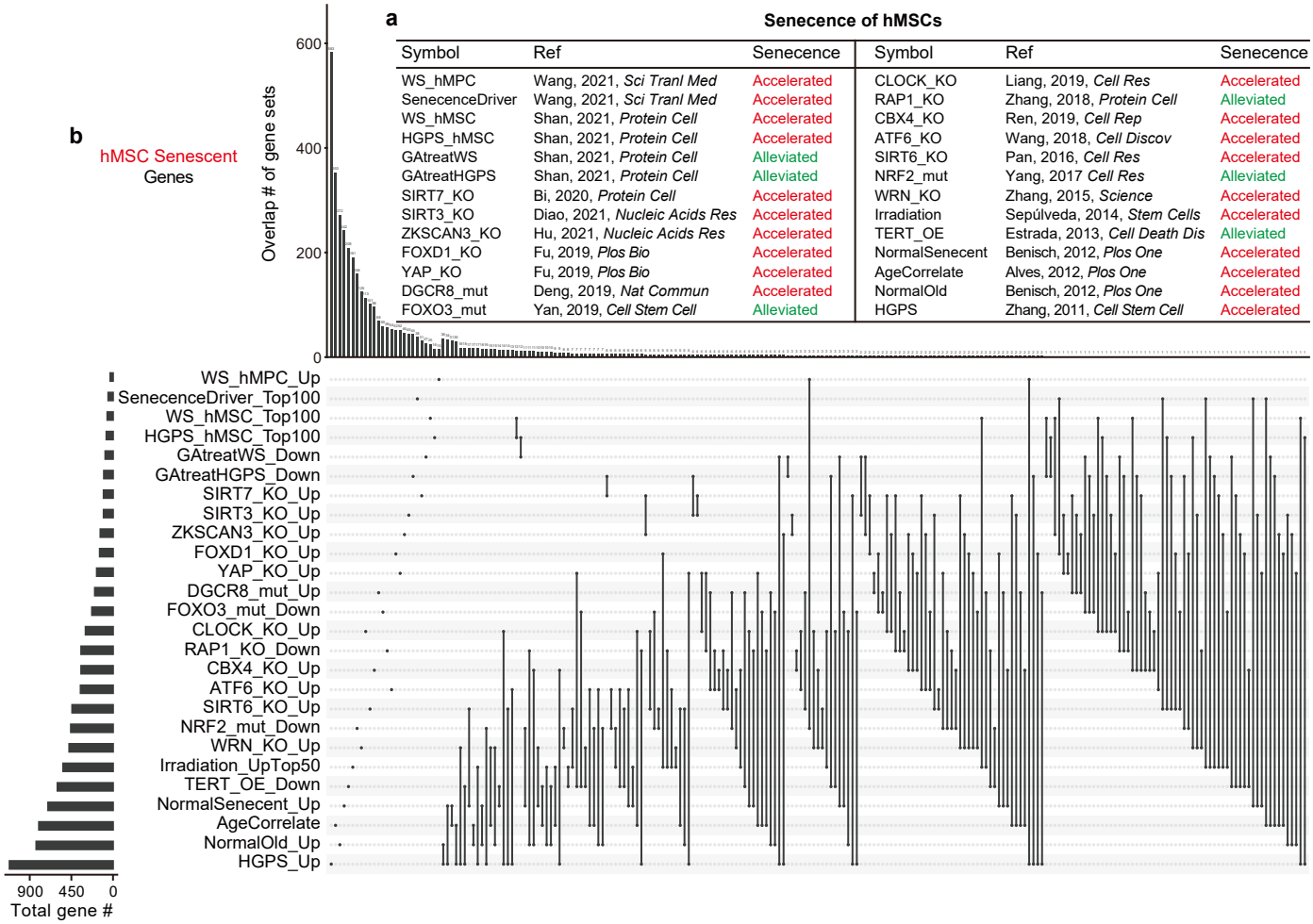

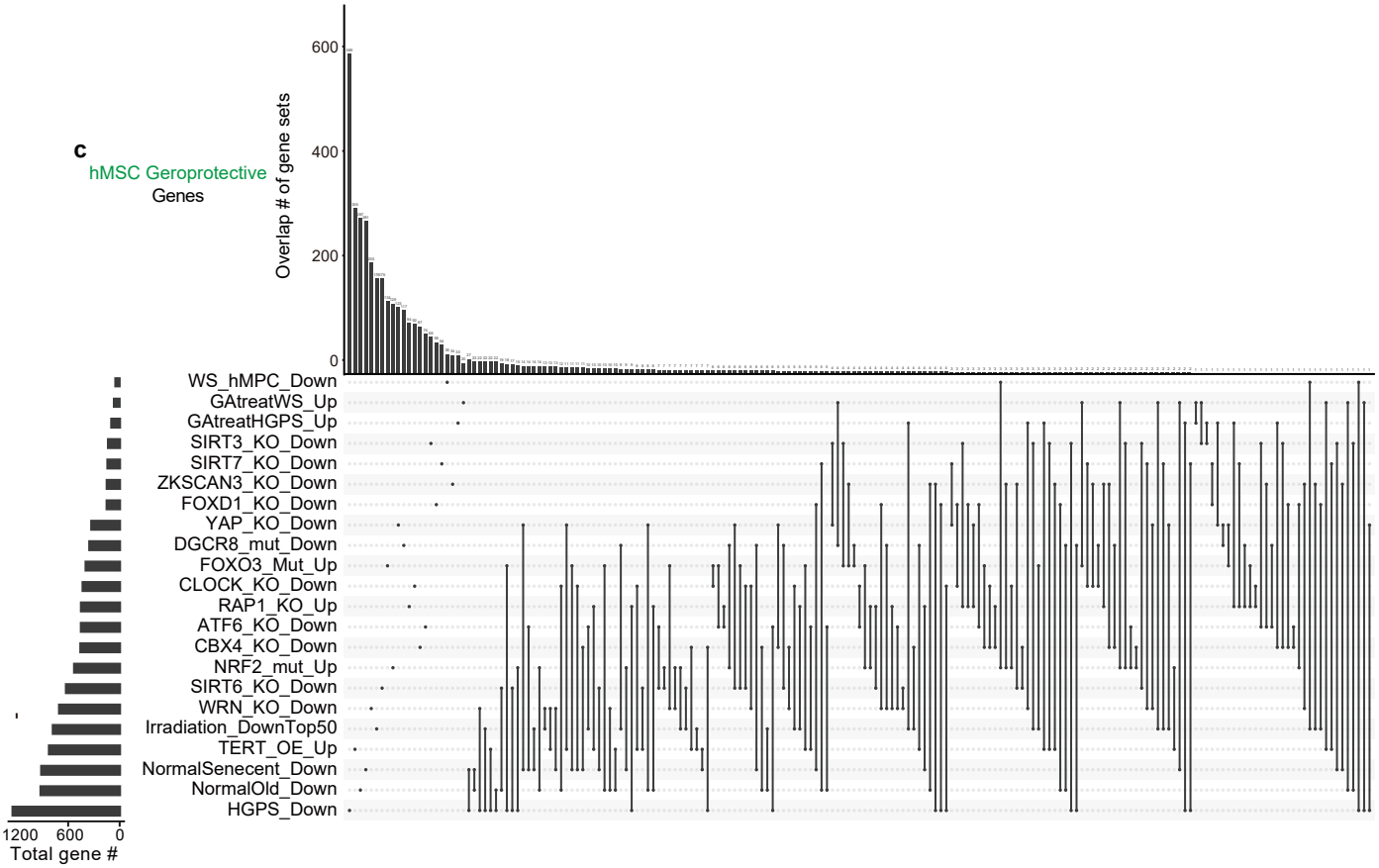

d

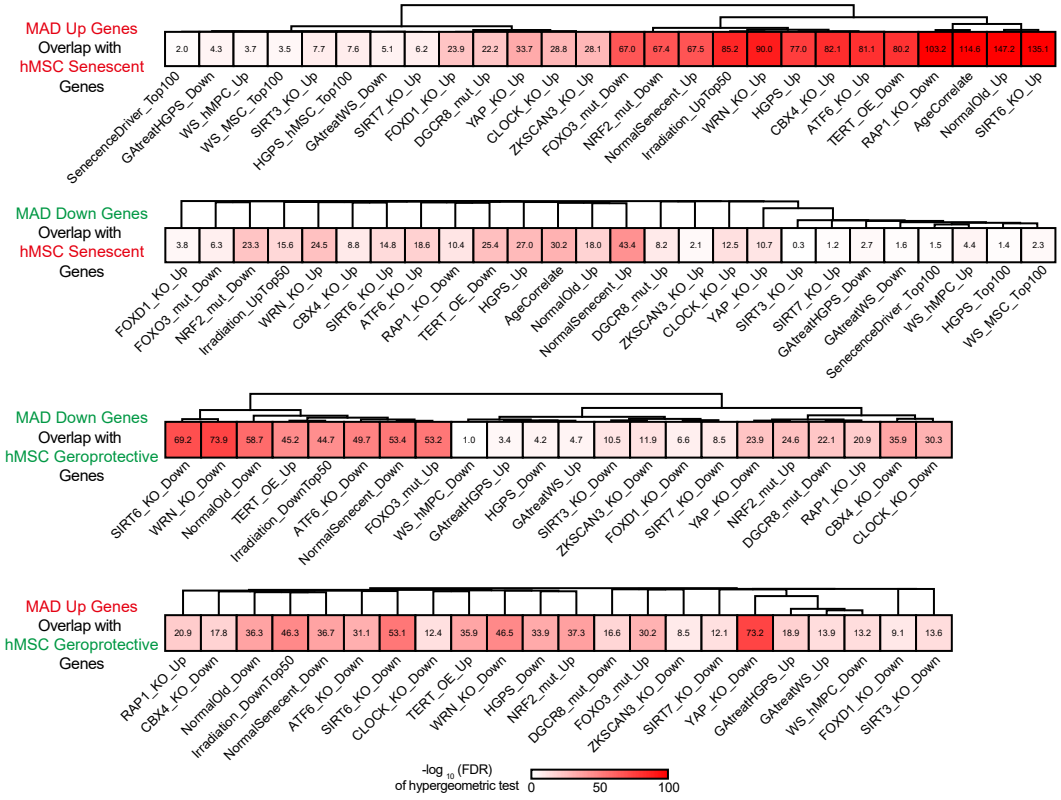
MAD Up Genes
Overlap with
hMSC Senescent
Genes
2.0 4.3 3.7 3.5 7.7 7.6 5.1 6.2 23.9 22.2 33.7 28.8 28.1 67.0 67.4 67.5 85.2 90.0 77.0 82.1 81.1 80.2 103.2 114.6 147.2 135.1
SenescenceDriver_Top100
GAtreatHGPS_Down
WS_hMPC_Up
WS_MSC_Top100
SIRT3_KO_Up
HGPS_hMSC_Top100
GAtreatWS_Down
SIRT7_KO_Up
FOXD1_KO_Up
DGCR8_mut_Up
YAP_KO_Up
CLOCK_KO_Up
ZKSCAN3_KO_Up
FOXO3_mut_Down
NRF2_mut_Down
NormalSenecent_Up
Irradiation_UpTop50
WRN_KO_Up
HGPS_Up
CBX4_KO_Up
ATF6_KO_Up
TERT_OE_Down
RAP1_KO_Down
AgeCorrelate
NormalOld_Up
SIRT6_KO_Up
MAD Down Genes
Overlap with
hMSC Senescent
Genes
3.8 6.3 23.3 15.6 24.5 8.8 14.8 18.6 10.4 25.4 27.0 30.2 18.0 43.4 8.2 2.1 12.5 10.7 0.3 1.2 2.7 1.6 1.5 4.4 1.4 2.3
FOXD1_KO_Up
FOXO3_mut_Down
NRF2_mut_Down
Irradiation_UpTop50
WRN_KO_Up
CBX4_KO_Up
SIRT6_KO_Up
ATF6_KO_Up
RAP1_KO_Down
TERT_OE_Down
HGPS_Up
AgeCorrelate
NormalOld_Up
NormalSenecent_Up
DGCR8_mut_Up
ZKSCAN3_KO_Up
CLOCK_KO_Up
YAP_KO_Up
SIRT3_KO_Up
SIRT7_KO_Up
GAtreatHGPS_Down
GAtreatWS_Down
SenescenceDriver_Top100
WS_hMPC_Up
HGPS_Top100
WS_MSC_Top100
MAD Down Genes
Overlap with
hMSC Geroprotective
Genes
69.2 73.9 58.7 45.2 44.7 49.7 53.4 53.2 1.0 3.4 4.2 4.7 10.5 11.9 6.6 8.5 23.9 24.6 22.1 20.9 35.9 30.3
SIRT6_KO_Down
WRN_KO_Down
NormalOld_Down
TERT_OE_Up
Irradiation_DownTop50
ATF6_KO_Down
NormalSenecent_Down
FOXO3_mut_Up
WS_hMPC_Down
GAtreatHGPS_Up
HGPS_Down
GAtreatWS_Up
SIRT3_KO_Down
ZKSCAN3_KO_Down
FOXD1_KO_Down
SIRT7_KO_Down
YAP_KO_Down
NRF2_mut_Up
DGCR8_mut_Down
RAP1_KO_Up
CBX4_KO_Down
CLOCK_KO_Down
MAD Up Genes
Overlap with
hMSC Geroprotective
Genes
20.9 17.8 36.3 46.3 36.7 31.1 53.1 12.4 35.9 46.5 33.9 37.3 16.6 30.2 8.5 12.1 73.2 18.9 13.9 13.2 9.1 13.6
RAP1_KO_Up
CBX4_KO_Down
NormalOld_Down
Irradiation_DownTop50
NormalSenecent_Down
ATF6_KO_Down
SIRT6_KO_Down
CLOCK_KO_Down
TERT_OE_Up
WRN_KO_Down
HGPS_Down
NRF2_mut_Up
DGCR8_mut_Down
FOXO3_mut_Up
ZKSCAN3_KO_Down
SIRT7_KO_Down
YAP_KO_Down
GAtreatHGPS_Up
GAtreatWS_Up
WS_hMPC_Down
FOXD1_KO_Down
SIRT3_KO_Down
-log 10 (FDR)
of hypergeometric test
0
50
100

Supplementary Fig. 8| Cross-analysis of hMSCs aging transcriptomes with MAD-MSCs. a, Summary of used human MSCs aging models, including 20 accelerated and 6 alleviated aging hMSCs transcriptomes. Relevant reference paper and senescence state are indicated. b, Cross-analysis of senescence-associated genes in the transcriptomes from different hMSCs aging models. c, Cross-analysis of geroprotection-associated genes in the transcriptomes from different hMSCs aging models. d, Cross-analysis of senescence/geroprotection associated profile enrichment in the transcriptomes from different hMSCs aging models.

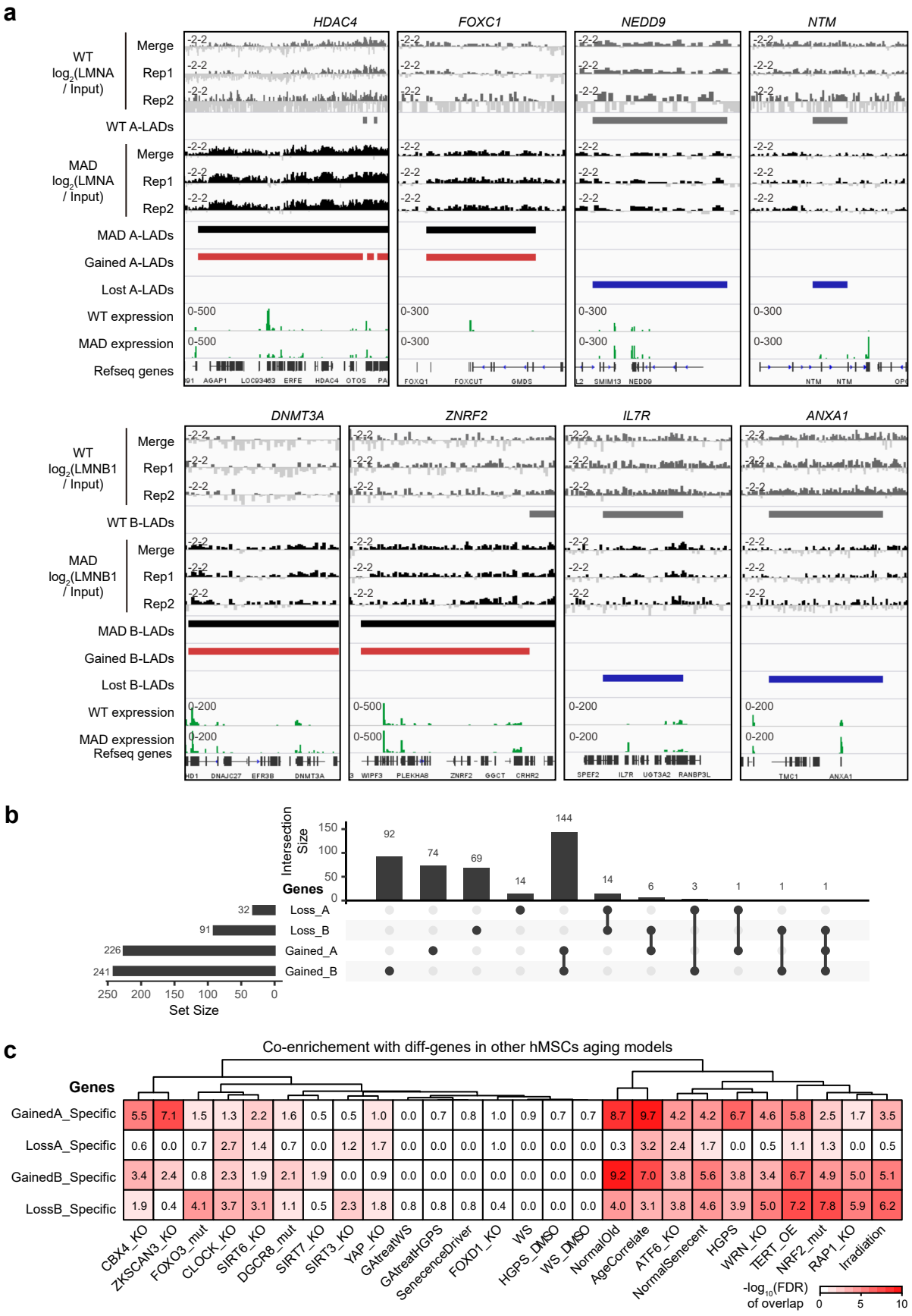
a
HDAC4
FOXC1
NEDD9
NTM
WT log2(LMNA / Input)
Merge
Rep1
Rep2
WT A-LADs
MAD log2(LMNA / Input)
MAD A-LADs
Gained A-LADs
Lost A-LADs
WT expression
MAD expression
Refseq genes
DNMT3A
ZNRF2
IL7R
ANXA1
WT log2(LMNB1 / Input)
WT B-LADs
MAD log2(LMNB1 / Input)
MAD B-LADs
Gained B-LADs
Lost B-LADs
b
Intersection Size
Genes
Loss_A
Loss_B
Gained_A
Gained_B
Set Size
c
Co-enrichement with diff-genes in other hMSCs aging models
Genes
GainedA_Specific
LossA_Specific
GainedB_Specific
LossB_Specific
CBX4_KO
ZKSCAN3_KO
FOXO3_mut
CLOCK_KO
SIRT6_KO
DGCR8_mut
SIRT7_KO
SIRT3_KO
YAP_KO
GAtreatWS
GAtreatHGPS
SenescenceDriver
FOXD1_KO
WS
HGPS_DMSO
WS_DMSO
NormalOld
AgeCorrelate
ATF6_KO
NormalSenecent
HGPS
WRN_KO
TERT_OE
NRF2_mut
RAP1_KO
Irradiation
-log10(FDR) of overlap

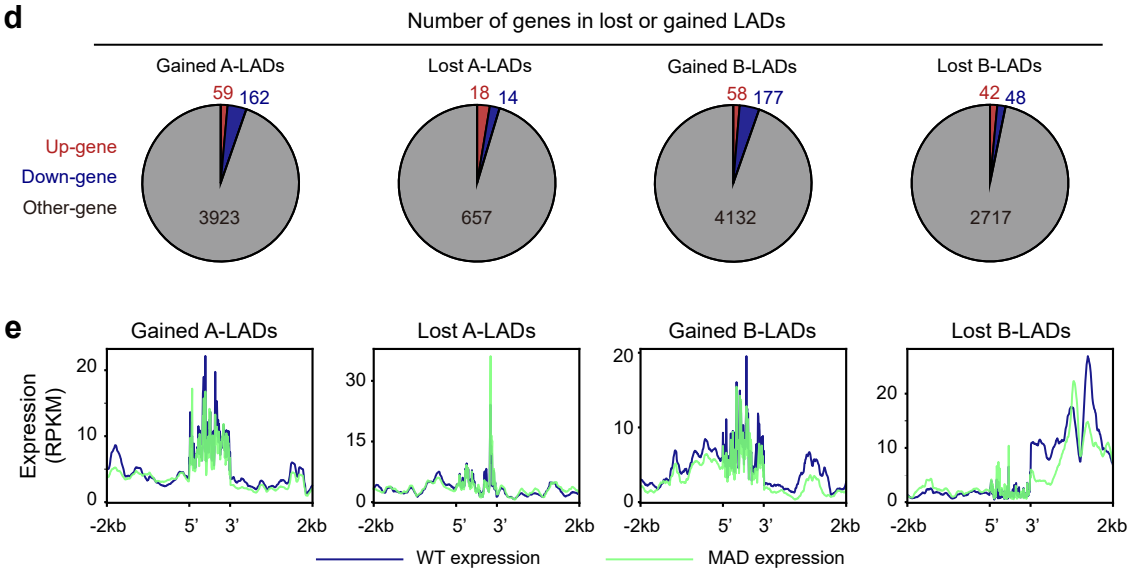
d
Number of genes in lost or gained LADs
Gained A-LADs
Lost A-LADs
Gained B-LADs
Lost B-LADs
Up-gene
Down-gene
Other-gene
59
162
3923
18
14
657
58
177
4132
42
48
2717
e
Gained A-LADs
Lost A-LADs
Gained B-LADs
Lost B-LADs
Expression (RPKM)
-2kb
5'
3'
2kb
WT expression
MAD expression

Supplementary Fig. 9| Reorganization of A and B lamina-associated domain in MAD-MSCs. a, Representative LADs reorganization and changes in gene expression. b, Intersection of changed gene sets linked to lost and gained A/B-LADs categories. c, The enrichment between the unique dysregulated genes specific to A- or B-LADs reorganization in MAD-MSCs and geroprotection/senescence-associated profiles in different hMSCs aging models. Color depth indicated enrichment score. d, Pie charts showing the summary of the number of genes in the gained and lost LADs. e, Average plots showing average gene expression in the indicated domains. The y-axis values represented RPKM.

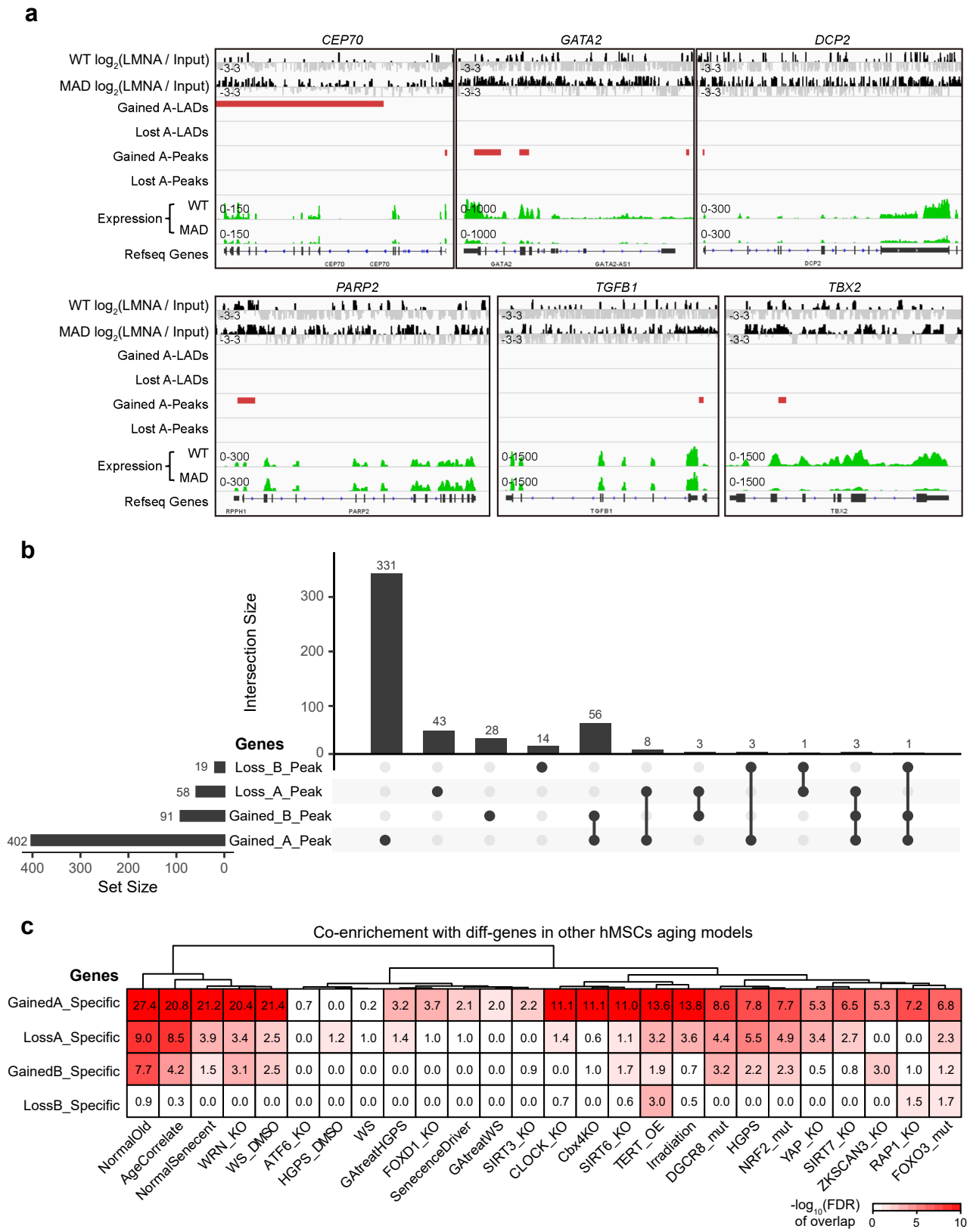
a
CEP70
GATA2
DCP2
WT log2(LMNA / Input)
MAD log2(LMNA / Input)
Gained A-LADs
Lost A-LADs
Gained A-Peaks
Lost A-Peaks
Expression
WT
MAD
Refseq Genes
0-150
0-1000
0-300
PARP2
TGFB1
TBX2
0-1500
b
Intersection Size
Genes
Loss_B_Peak
Loss_A_Peak
Gained_B_Peak
Gained_A_Peak
Set Size
c
Co-enrichement with diff-genes in other hMSCs aging models
GainedA_Specific
LossA_Specific
GainedB_Specific
LossB_Specific
NormalOld
AgeCorrelate
NormalSenecent
WRN_KO
WS_DMSO
ATF6_KO
HGPS_DMSO
WS
GAtreatHGPS
FOXD1_KO
SenecenceDriver
GAtreatWS
SIRT3_KO
CLOCK_KO
Cbx4KO
SIRT6_KO
TERT_OE
Irradiation
DGCR8_mut
HGPS
NRF2_mut
YAP_KO
SIRT7_KO
ZKSCAN3_KO
RAP1_KO
FOXO3_mut
-log10(FDR) of overlap

Supplementary Fig. 10| Reposition of A and B non-LAD lamina-chromatin binding peaks in MAD-MSCs. a, Representative reposition of non-LAD lamina-chromatin binding peaks and changes in gene expression. b, Intersection of changed gene sets correlated with repositioned non-LAD lamina-chromatin binding. c, The enrichment between the unique dysregulated genes specific to repositioned non-LADs lamina-chromatin binding in MAD-MSCs and geroprotection/senescence-associated profile in different hMSCs aging models. Color depth indicates the enrichment score.

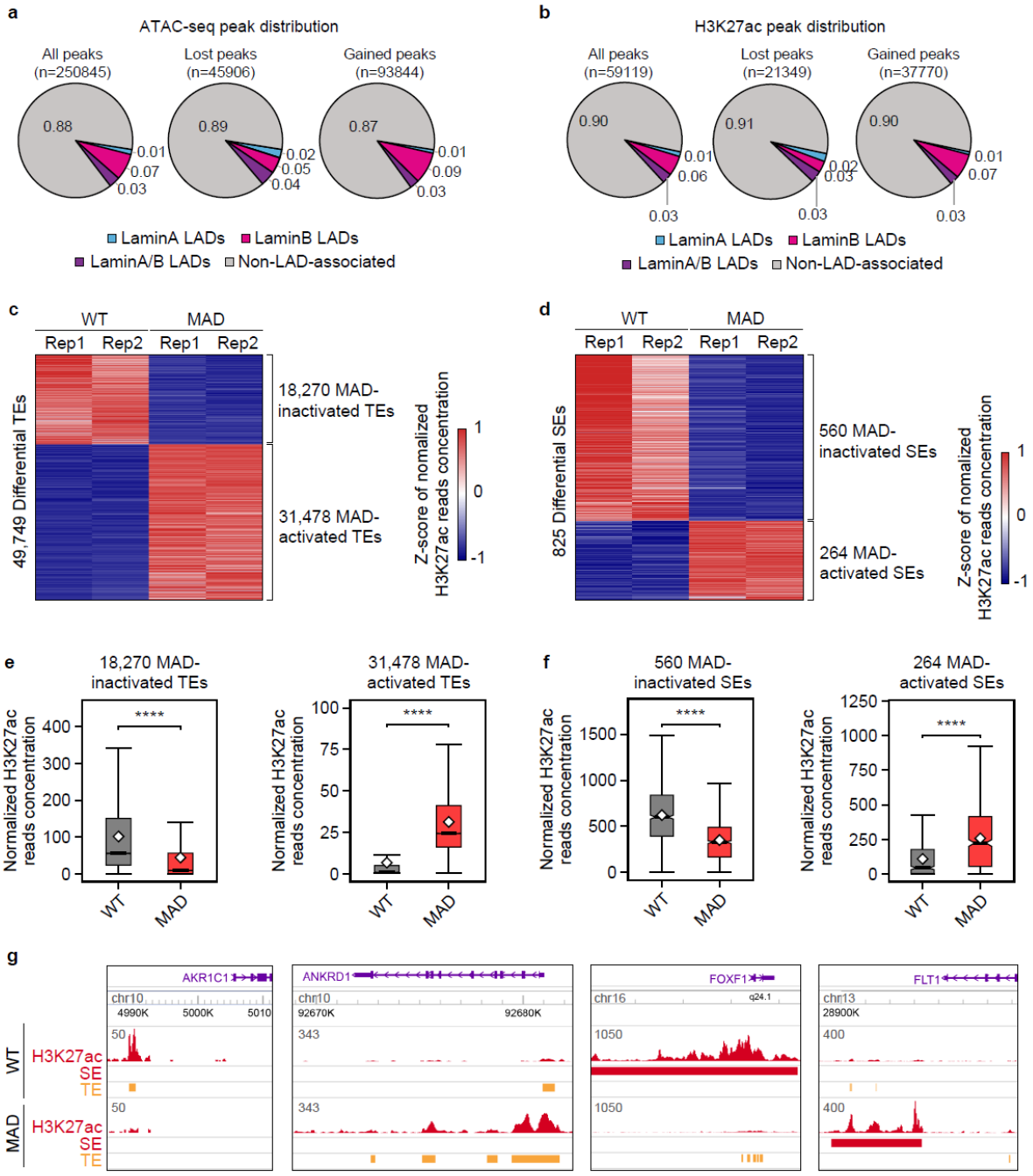
a
ATAC-seq peak distribution
All peaks (n=250845)
Lost peaks (n=45906)
Gained peaks (n=93844)
0.88
0.01
0.07
0.03
0.89
0.02
0.05
0.04
0.87
0.01
0.09
0.03
LaminA LADs
LaminB LADs
LaminA/B LADs
Non-LAD-associated
b
H3K27ac peak distribution
All peaks (n=59119)
Lost peaks (n=21349)
Gained peaks (n=37770)
0.90
0.01
0.06
0.03
0.91
0.02
0.03
0.03
0.90
0.01
0.07
0.03
LaminA LADs
LaminB LADs
LaminA/B LADs
Non-LAD-associated
c
WT
MAD
Rep1
Rep2
Rep1
Rep2
49,749 Differential TEs
18,270 MAD-inactivated TEs
31,478 MAD-activated TEs
Z-score of nomalized H3K27ac reads concentration
1
0
-1
d
WT
MAD
Rep1
Rep2
Rep1
Rep2
825 Differential SEs
560 MAD-inactivated SEs
264 MAD-activated SEs
Z-score of nomalized H3K27ac reads concentration
1
0
-1
e
18,270 MAD-inactivated TEs
Normalized H3K27ac reads concentration
400
300
200
100
0
****
WT
MAD
31,478 MAD-activated TEs
Normalized H3K27ac reads concentration
100
75
50
25
0
****
WT
MAD
f
560 MAD-inactivated SEs
Normalized H3K27ac reads concentration
1500
1000
500
0
****
WT
MAD
264 MAD-activated SEs
Normalized H3K27ac reads concentration
1250
1000
750
500
250
0
****
WT
MAD
g
AKR1C1
chr10
4990K
5000K
5010
ANKRD1
chr10
92670K
92680K
FOXF1
chr16
q24.1
FLT1
chr13
28900K
WT
MAD
H3K27ac
SE
TE
50
343
1050
400

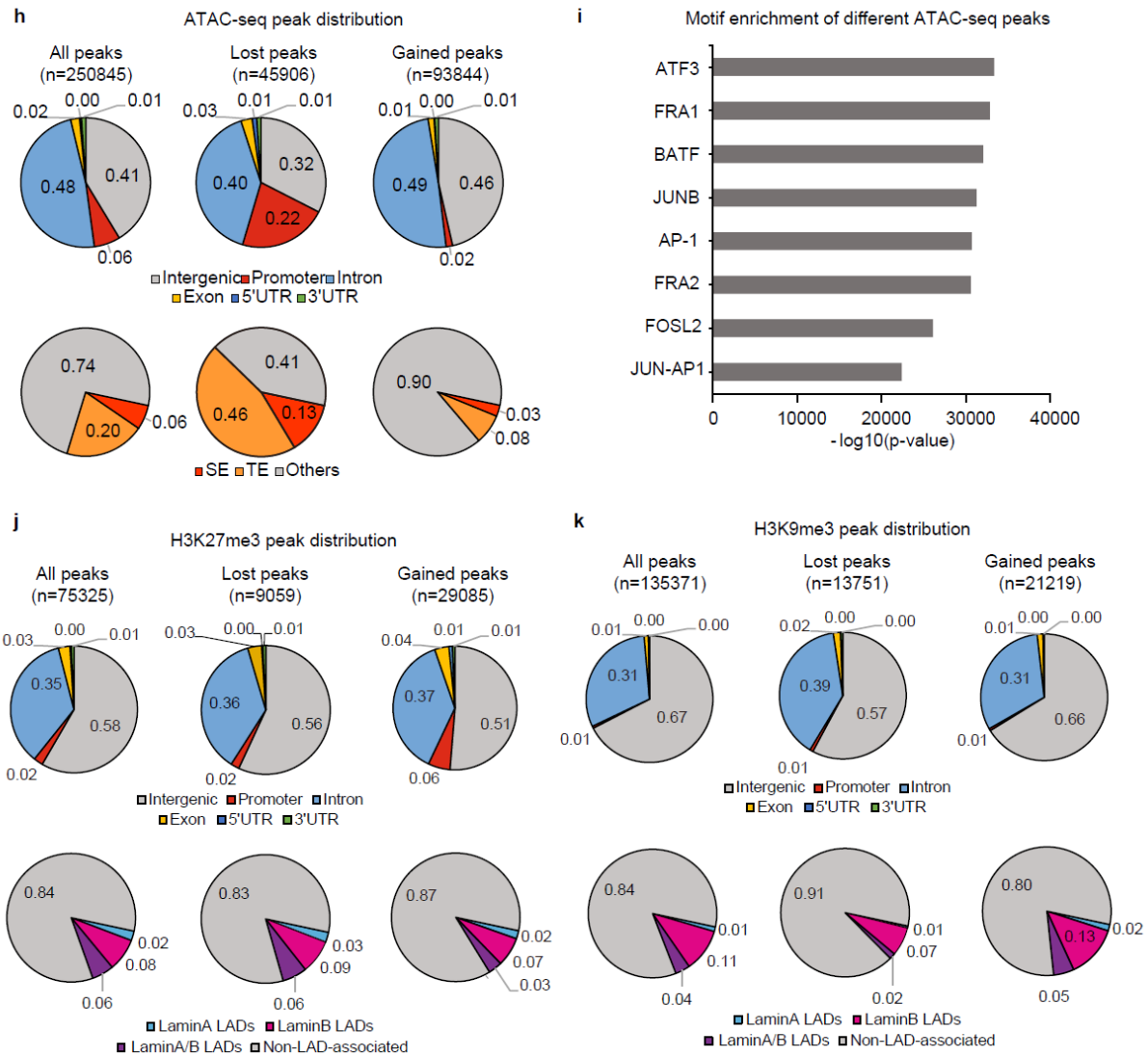
h
ATAC-seq peak distribution
All peaks (n=250845)
Lost peaks (n=45906)
Gained peaks (n=93844)
0.02 0.00 0.01 0.48 0.41 0.06
0.03 0.01 0.01 0.40 0.32 0.22
0.01 0.00 0.01 0.49 0.46 0.02
Intergenic Promoter Intron
Exon 5'UTR 3'UTR
0.74 0.20 0.06
0.41 0.46 0.13
0.90 0.03 0.08
SE TE Others
i
Motif enrichment of different ATAC-seq peaks
ATF3
FRA1
BATF
JUNB
AP-1
FRA2
FOSL2
JUN-AP1
0 10000 20000 30000 40000
-log10(p-value)
j
H3K27me3 peak distribution
All peaks (n=75325)
Lost peaks (n=9059)
Gained peaks (n=29085)
0.03 0.00 0.01 0.35 0.58 0.02
0.03 0.00 0.01 0.36 0.56 0.02
0.04 0.01 0.01 0.37 0.51 0.06
Intergenic Promoter Intron
Exon 5'UTR 3'UTR
0.84 0.02 0.08 0.06
0.83 0.03 0.09 0.06
0.87 0.02 0.07 0.03
LaminA LADs LaminB LADs
LaminA/B LADs Non-LAD-associated
k
H3K9me3 peak distribution
All peaks (n=135371)
Lost peaks (n=13751)
Gained peaks (n=21219)
0.01 0.00 0.00 0.31 0.67 0.01
0.02 0.00 0.00 0.39 0.57 0.01
0.01 0.00 0.00 0.31 0.66 0.01
Intergenic Promoter Intron
Exon 5'UTR 3'UTR
0.84 0.01 0.11 0.04
0.91 0.01 0.07 0.02
0.80 0.13 0.02 0.05
LaminA LADs LaminB LADs
LaminA/B LADs Non-LAD-associated

Supplementary Fig. 11| Distribution of chromatin modifications and lamina-chromatin interaction in MAD-MSCs. a, The distribution of ATAC peaks within and beyond A-/B-LADs. b, The distribution of H3K27ac peaks within and beyond A-/B-LADs. c-d, Heatmaps of differential typical enhancers (TEs) and super enhancers (SEs). e-f, Annotation of active and inactive TEs/SEs in MAD-MSCs. g, Representative genes with active and inactive TEs and SEs in MAD-MSCs. h, Global ATAC peaks distribution and their correlation with TEs and SEs. i, HOMER transcription factor motif enrichment analysis of ATAC peaks. j-k, Global distribution of H3K27me3 and H3K9me3 peaks and their relationship with A-/B-LADs. All p-values were determined using the two-sided Wilcoxon rank-sum test.

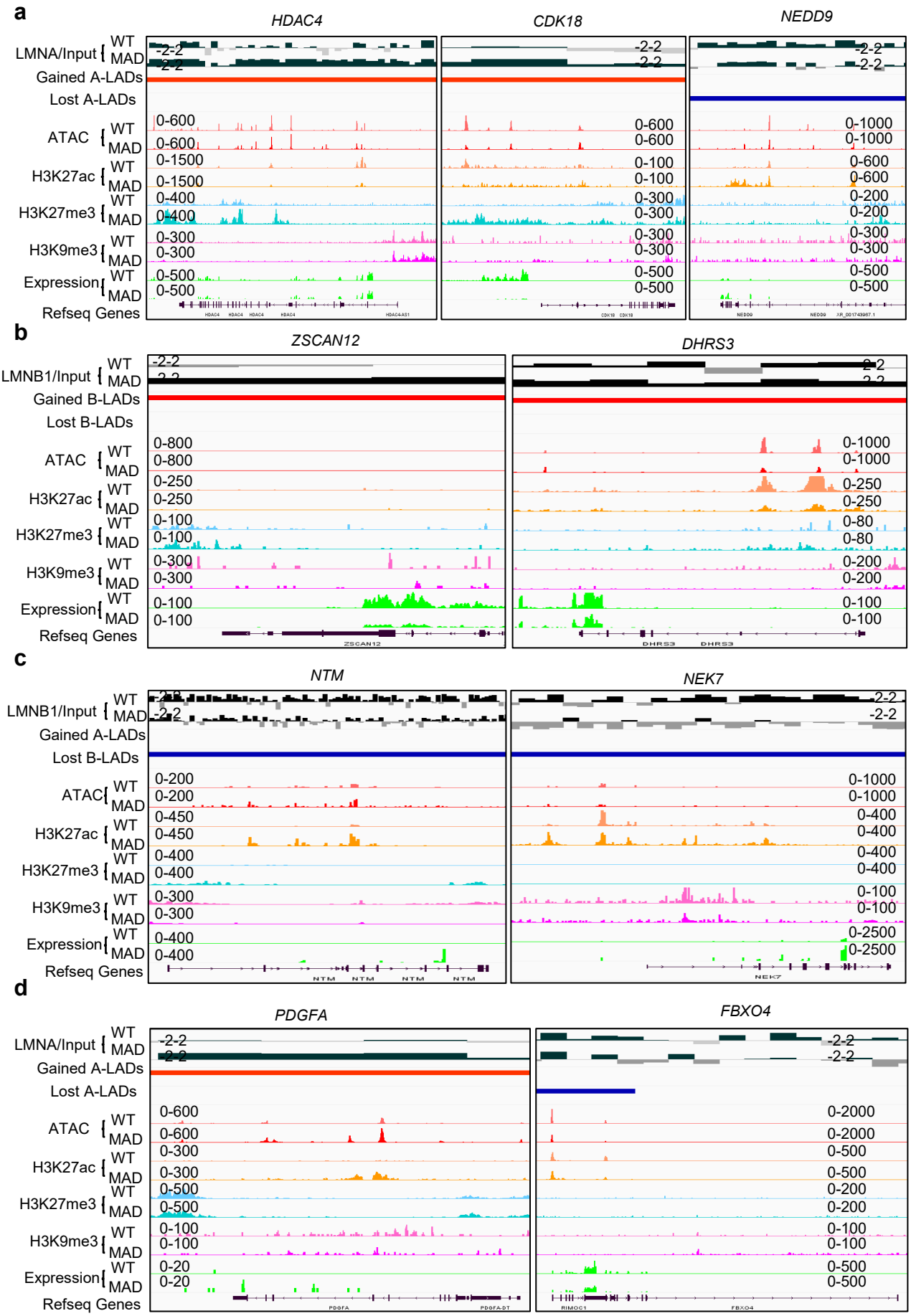
a
HDAC4
CDK18
NEDD9
LMNA/Input
WT
MAD
Gained A-LADs
Lost A-LADs
ATAC
H3K27ac
H3K27me3
H3K9me3
Expression
Refseq Genes
b
ZSCAN12
DHRS3
LMNB1/Input
Gained B-LADs
Lost B-LADs
c
NTM
NEK7
d
PDGFA
FBXO4

Supplementary Fig. 12| Integrated analysis of chromatin features and LADs reorganization. a-b, Representative gene regulation by coordinated control of chromatin features and A-LADs reorganization. c-d, Representative gene regulation by coordinated control of chromatin features and B-LADs reorganization.

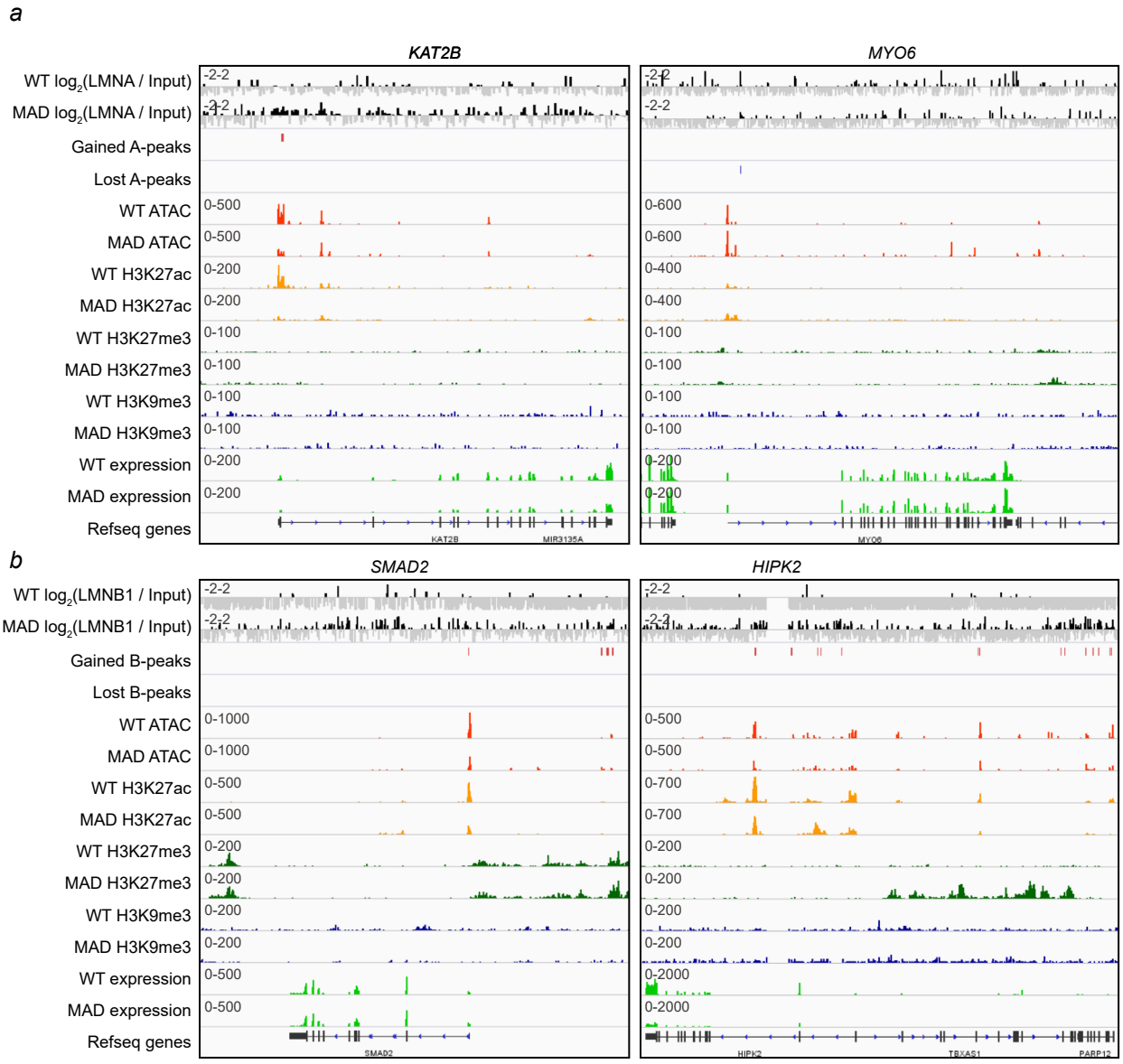
a
KAT2B
MYO6
WT log2(LMNA / Input)
MAD log2(LMNA / Input)
Gained A-peaks
Lost A-peaks
WT ATAC
MAD ATAC
WT H3K27ac
MAD H3K27ac
WT H3K27me3
MAD H3K27me3
WT H3K9me3
MAD H3K9me3
WT expression
MAD expression
Refseq genes
b
SMAD2
HIPK2
WT log2(LMNB1 / Input)
MAD log2(LMNB1 / Input)
Gained B-peaks
Lost B-peaks
WT ATAC
MAD ATAC
WT H3K27ac
MAD H3K27ac
WT H3K27me3
MAD H3K27me3
WT H3K9me3
MAD H3K9me3
WT expression
MAD expression
Refseq genes

Supplementary Fig. 13| Integrated analysis of chromatin features and repositioned non-LAD lamina-chromatin binding peaks. a, Representative gene regulation by coordinated control of chromatin features and reposition of A-type non-LAD lamina-chromatin binding peaks. b, Representative gene regulation by coordinated control of chromatin features and reposition of B-type non-LAD lamina-chromatin binding peaks.

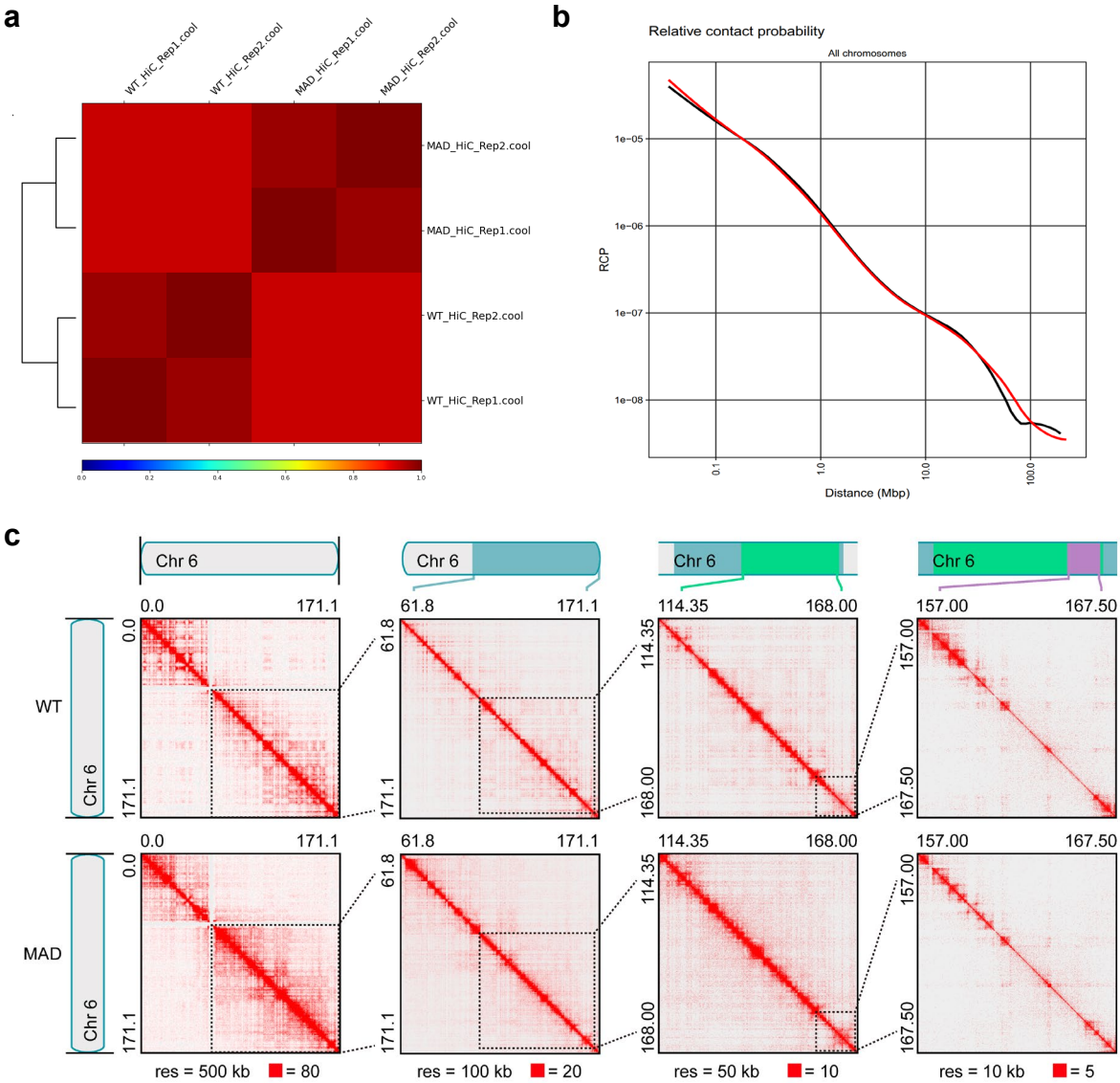
a
WT_HiC_Rep1.cool
WT_HiC_Rep2.cool
MAD_HiC_Rep1.cool
MAD_HiC_Rep2.cool
b
Relative contact probability
All chromosomes
RCP
Distance (Mbp)
c
Chr 6
WT
MAD
res = 500 kb
= 80
res = 100 kb
= 20
res = 50 kb
= 10
res = 10 kb
= 5
d
Non-switched A/B
A>B Switch
B>A Switch
Filtered
9.96%
14.36%
4.66%
71.04%
10.34%
12.83%
9.88%
8.17%
9.39%
20.43%
Stable A
Stengthened A
Weakened A
Stable B
Stengthened B
Weakened B

Supplementary Fig. 14| Hierarchical chromatin structure change in MAD-MSCs. a, Normalized heatmap of HiC data obtained from WT-MSCs and MAD-MSCs with two replicates. b, Analysis of relative contact probability (RCP) at different distance cross chromosome. c, Zoomed-in views of the representative interaction heatmaps at specific genomic region in WT-MSCs and MAD-MSCs (500-kb, 100-kb, 50-kb and 10-kb bin). d, Percentage of compartment A/B switch in MAD-MSCs, compared to WT-MSCs.

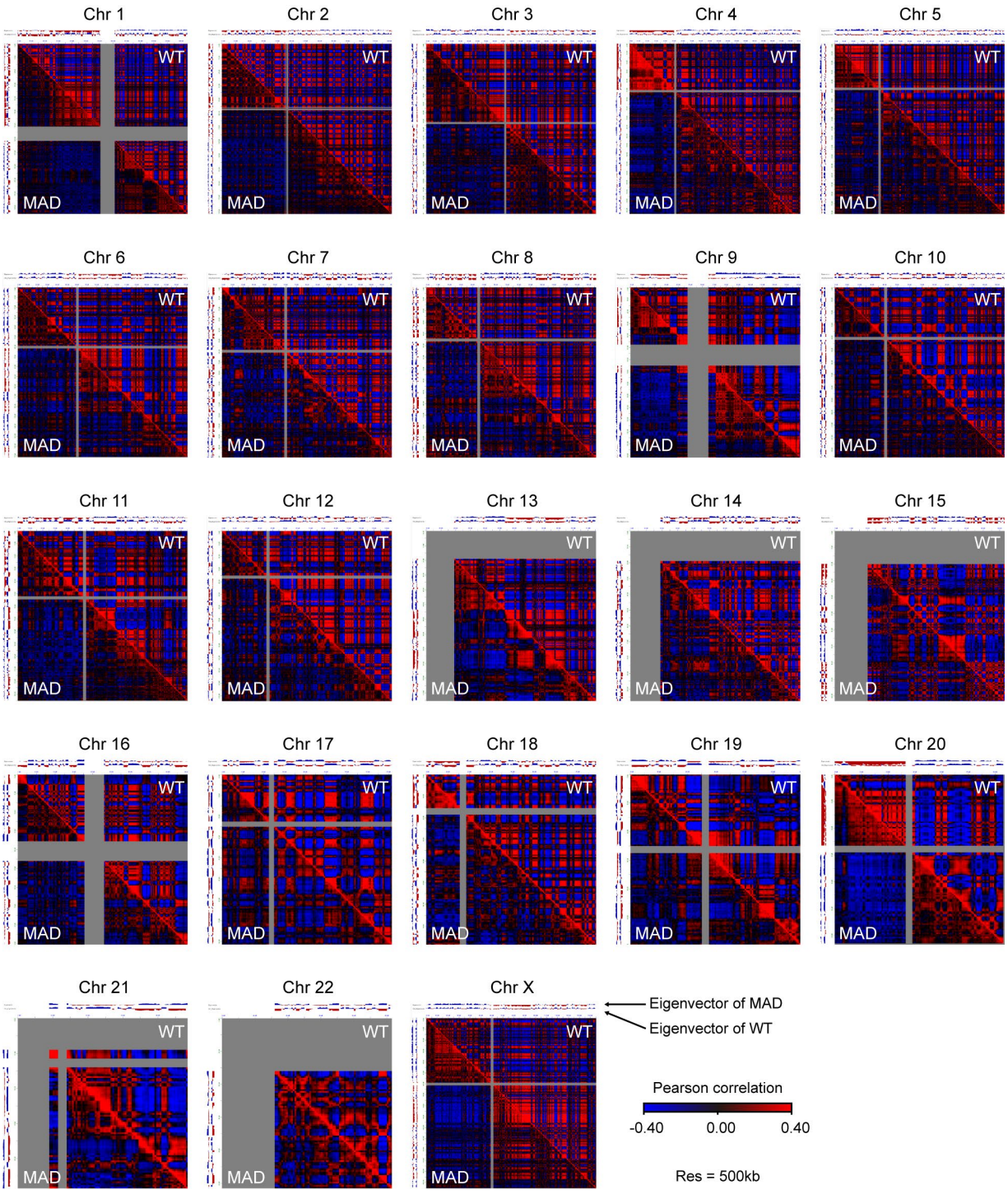
Chr 1
Chr 2
Chr 3
Chr 4
Chr 5
Chr 6
Chr 7
Chr 8
Chr 9
Chr 10
Chr 11
Chr 12
Chr 13
Chr 14
Chr 15
Chr 16
Chr 17
Chr 18
Chr 19
Chr 20
Chr 21
Chr 22
Chr X
WT
MAD
Eigenvector of MAD
Eigenvector of WT
Pearson correlation
-0.40
0.00
0.40
Res = 500kb

Supplementary Fig. 15| Global decreased chromatin compartmentalization in MAD-MSCs. Compartmentalization analysis of each chromosome in WT-MSCs and MAD-MSCs.

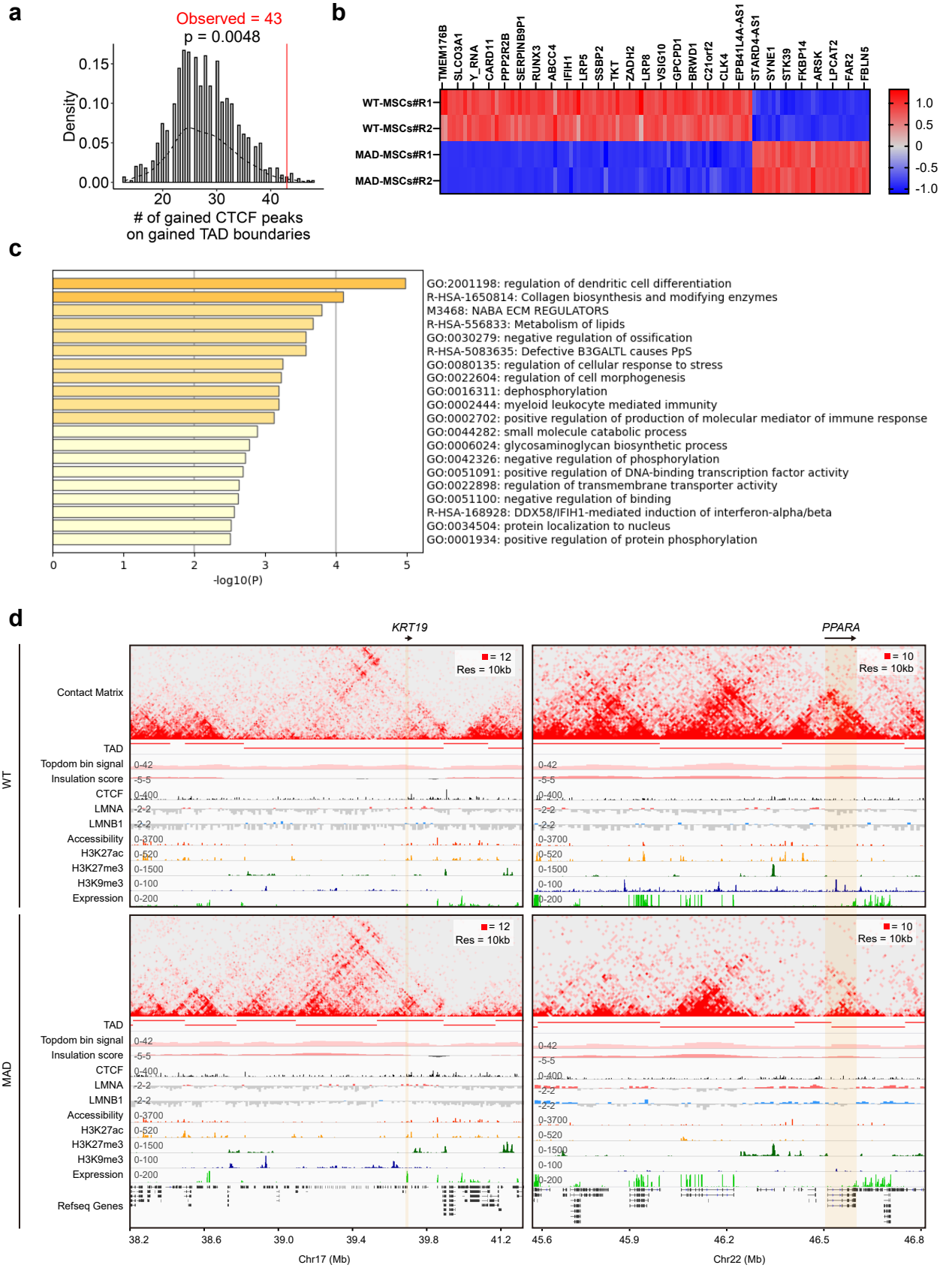
a
Observed = 43
p = 0.0048
Density
0.15
0.10
0.05
0.00
20
30
40
# of gained CTCF peaks
on gained TAD boundaries
b
TMEM176B
SLCO3A1
Y_RNA
CARD11
PPP2R2B
SERPINB9P1
RUNX3
ABCC4
IFIH1
LRP5
SSBP2
TKT
ZADH2
LRP8
VSIG10
GPCPD1
BRWD1
C21orf2
CLK4
EPB41L4A-AS1
STARD4-AS1
SYNE1
STK39
FKBP14
ARSK
LPCAT2
FAR2
FBLN5
WT-MSCs#R1
WT-MSCs#R2
MAD-MSCs#R1
MAD-MSCs#R2
1.0
0.5
0
-0.5
-1.0
c
GO:2001198: regulation of dendritic cell differentiation
R-HSA-1650814: Collagen biosynthesis and modifying enzymes
M3468: NABA ECM REGULATORS
R-HSA-556833: Metabolism of lipids
GO:0030279: negative regulation of ossification
R-HSA-5083635: Defective B3GALTL causes PpS
GO:0080135: regulation of cellular response to stress
GO:0022604: regulation of cell morphogenesis
GO:0016311: dephosphorylation
GO:0002444: myeloid leukocyte mediated immunity
GO:0002702: positive regulation of production of molecular mediator of immune response
GO:0044282: small molecule catabolic process
GO:0006024: glycosaminoglycan biosynthetic process
GO:0042326: negative regulation of phosphorylation
GO:0051091: positive regulation of DNA-binding transcription factor activity
GO:0022898: regulation of transmembrane transporter activity
GO:0051100: negative regulation of binding
R-HSA-168928: DDX58/IFIH1-mediated induction of interferon-alpha/beta
GO:0034504: protein localization to nucleus
GO:0001934: positive regulation of protein phosphorylation
0
1
2
3
4
5
-log10(P)
d
KRT19
PPARA
WT
MAD
Contact Matrix
TAD
Topdom bin signal
Insulation score
CTCF
LMNA
LMNB1
Accessibility
H3K27ac
H3K27me3
H3K9me3
Expression
Refseq Genes
= 12
Res = 10kb
= 10
Res = 10kb
38.2
38.6
39.0
39.4
39.8
41.2
Chr17 (Mb)
45.6
45.9
46.2
46.5
46.8
Chr22 (Mb)

Supplementary Fig. 16| Gene dysregulation in shortened TADs and altered lamina-chromatin interaction regions. a, Permutated and observed CTCF bindings at the TAD boundaries in MAD-MSCs. b, Heatmap of dysregulated genes expression in shortened TADs and altered lamina-chromatin interaction regions. c, Enriched pathway of dysregulated transcription in shortened TADs and altered lamina-chromatin interaction regions. c, Representative dysregulated genes expression in shortened TADs. d, Representative genomic browser views of reorganized TADs in WT and MAD, including *KRT19* and *PPARA*. The y-axis values of lamina (LMNA or LMNB1) represented log2RPKM (Signal vs Input). The y-axis values of accessibility, histone modifications and expression represented RPKM. All p-values were determined using the two-sided Wilcoxon rank-sum test.

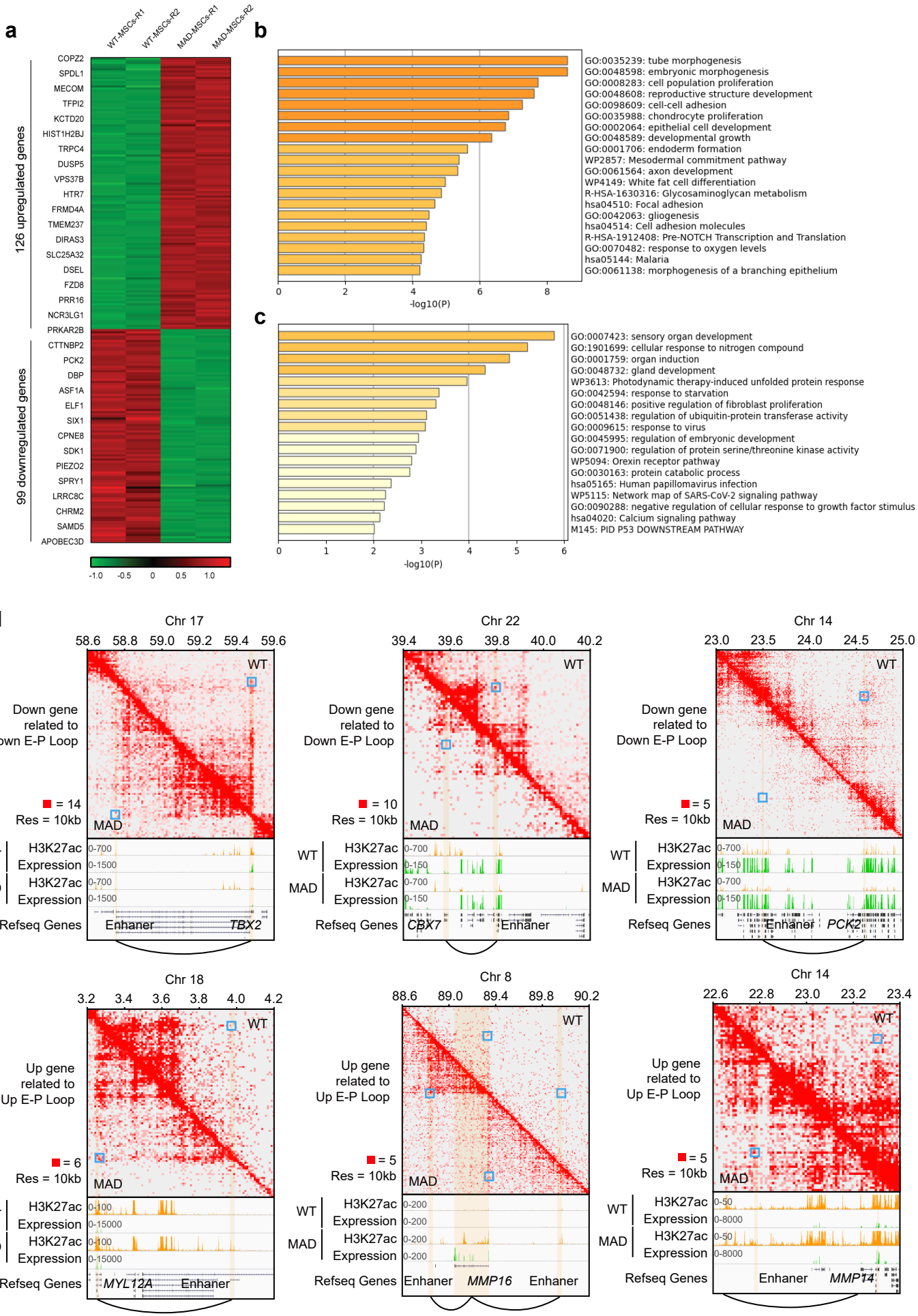
a
WT-MSCs-R1
WT-MSCs-R2
MAD-MSCs-R1
MAD-MSCs-R2
126 upregulated genes
99 downregulated genes
COPZ2
SPDL1
MECOM
TFPI2
KCTD20
HIST1H2BJ
TRPC4
DUSP5
VPS37B
HTR7
FRMD4A
TMEM237
DIRAS3
SLC25A32
DSEL
FZD8
PRR16
NCR3LG1
PRKAR2B
CTTNBP2
PCK2
DBP
ASF1A
ELF1
SIX1
CPNE8
SDK1
PIEZO2
SPRY1
LRRC8C
CHRM2
SAMD5
APOBEC3D
-1.0 -0.5 0 0.5 1.0
b
GO:0035239: tube morphogenesis
GO:0048598: embryonic morphogenesis
GO:0008283: cell population proliferation
GO:0048608: reproductive structure development
GO:0098609: cell-cell adhesion
GO:0035988: chondrocyte proliferation
GO:0002064: epithelial cell development
GO:0048589: developmental growth
GO:0001706: endoderm formation
WP2857: Mesodermal commitment pathway
GO:0061564: axon development
WP4149: White fat cell differentiation
R-HSA-1630316: Glycosaminoglycan metabolism
hsa04510: Focal adhesion
GO:0042063: gliogenesis
hsa04514: Cell adhesion molecules
R-HSA-1912408: Pre-NOTCH Transcription and Translation
GO:0070482: response to oxygen levels
hsa05144: Malaria
GO:0061138: morphogenesis of a branching epithelium
0 2 4 6 8
-log10(P)
c
GO:0007423: sensory organ development
GO:1901699: cellular response to nitrogen compound
GO:0001759: organ induction
GO:0048732: gland development
WP3613: Photodynamic therapy-induced unfolded protein response
GO:0042594: response to starvation
GO:0048146: positive regulation of fibroblast proliferation
GO:0051438: regulation of ubiquitin-protein transferase activity
GO:0009615: response to virus
GO:0045995: regulation of embryonic development
GO:0071900: regulation of protein serine/threonine kinase activity
WP5094: Orexin receptor pathway
GO:0030163: protein catabolic process
hsa05165: Human papillomavirus infection
WP5115: Network map of SARS-CoV-2 signaling pathway
GO:0090288: negative regulation of cellular response to growth factor stimulus
hsa04020: Calcium signaling pathway
M145: PID P53 DOWNSTREAM PATHWAY
0 1 2 3 4 5 6
-log10(P)
d
Chr 17
58.6 58.8 59.0 59.2 59.4 59.6
WT
Down gene related to Down E-P Loop
= 14
Res = 10kb
MAD
WT H3K27ac 0-700
Expression 0-1500
MAD H3K27ac 0-700
Expression 0-1500
Refseq Genes
Enhaner
TBX2
Chr 22
39.4 39.6 39.8 40.0 40.2
WT
Down gene related to Down E-P Loop
= 10
Res = 10kb
MAD
WT H3K27ac 0-700
Expression 0-150
MAD H3K27ac 0-700
Expression 0-150
Refseq Genes
CBX7
Enhaner
Chr 14
23.0 23.5 24.0 24.5 25.0
WT
Down gene related to Down E-P Loop
= 5
Res = 10kb
MAD
WT H3K27ac 0-700
Expression 0-150
MAD H3K27ac 0-700
Expression 0-150
Refseq Genes
Enhaner
PCK2
Chr 18
3.2 3.4 3.6 3.8 4.0 4.2
WT
Up gene related to Up E-P Loop
= 6
Res = 10kb
MAD
WT H3K27ac 0-100
Expression 0-15000
MAD H3K27ac 0-100
Expression 0-15000
Refseq Genes
MYL12A
Enhaner
Chr 8
88.6 89.0 89.4 89.8 90.2
WT
Up gene related to Up E-P Loop
= 5
Res = 10kb
MAD
WT H3K27ac 0-200
Expression 0-200
MAD H3K27ac 0-200
Expression 0-200
Refseq Genes
Enhaner
MMP16
Enhaner
Chr 14
22.6 22.8 23.0 23.2 23.4
WT
Up gene related to Up E-P Loop
= 5
Res = 10kb
MAD
WT H3K27ac 0-50
Expression 0-8000
MAD H3K27ac 0-50
Expression 0-8000
Refseq Genes
Enhaner
MMP14

Supplementary Fig. 17| Altered chromatin E-P loops dysregulate aging-associated genes. a, Heatmap of dysregulated genes expression in altered chromatin E-P loops. b-c, Enriched pathways of dysregulated transcription in altered chromatin E-P loops. d, Representative dysregulation of geroprotection- and senescence-associate genes in altered chromatin E-P loop. All p-values were determined using the two-sided Wilcoxon rank-sum test.

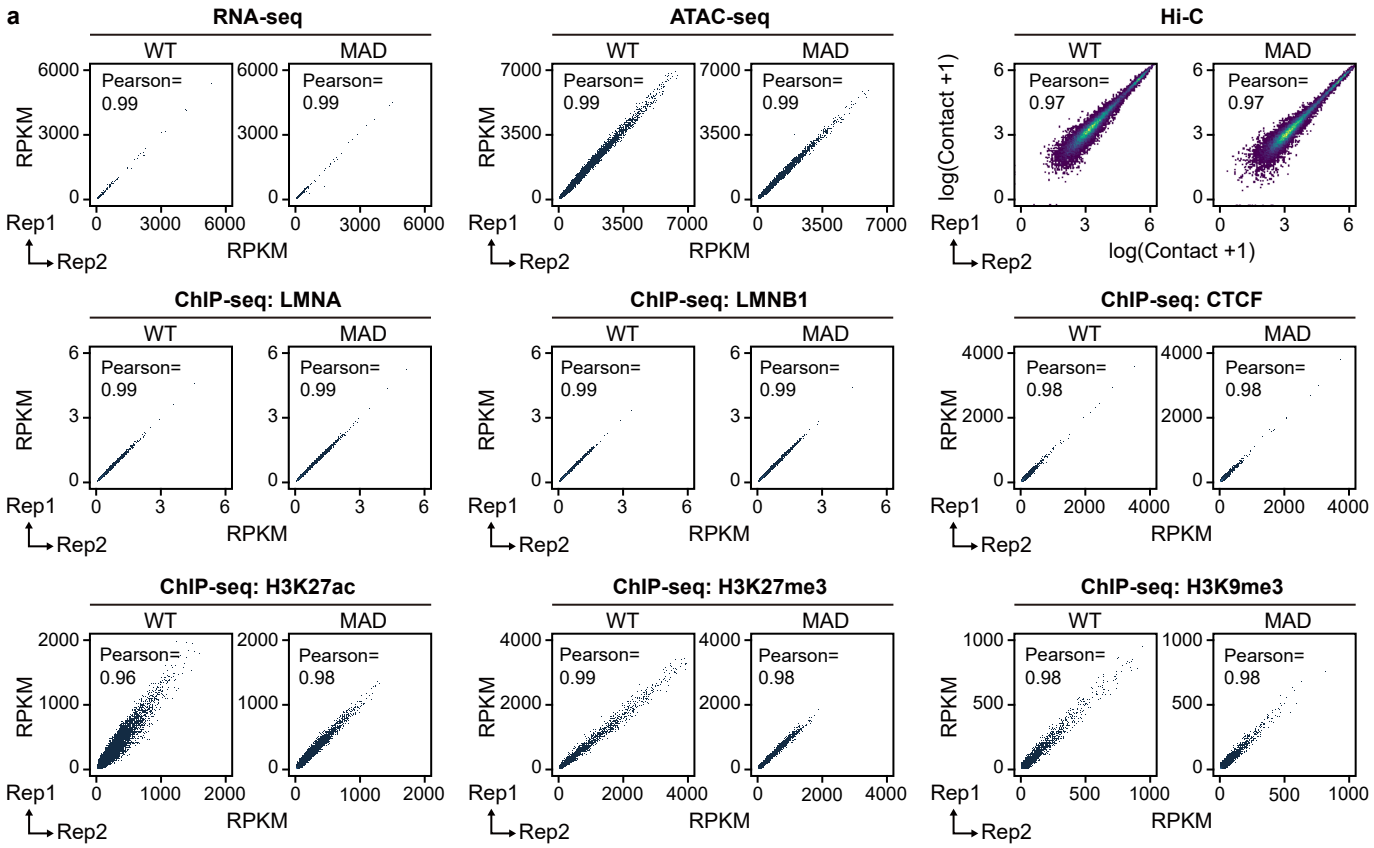
a
RNA-seq
ATAC-seq
Hi-C
ChIP-seq: LMNA
ChIP-seq: LMNB1
ChIP-seq: CTCF
ChIP-seq: H3K27ac
ChIP-seq: H3K27me3
ChIP-seq: H3K9me3
WT
MAD
Pearson= 0.99
Pearson= 0.97
Pearson= 0.98
Pearson= 0.96
RPKM
log(Contact +1)
Rep1
Rep2

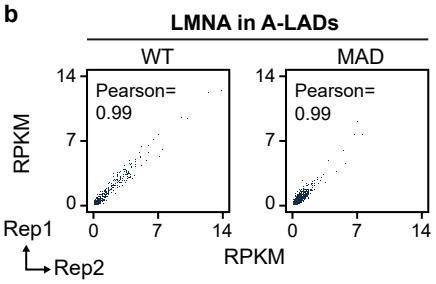
b
LMNA in A-LADs
LMNB1 in B-LADs
WT
MAD
Pearson= 0.99
RPKM
Rep1
Rep2

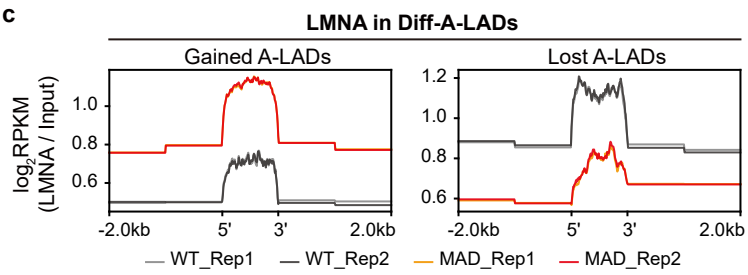
c
LMNA in Diff-A-LADs
LMNB1 in Diff-A-LADs
Gained A-LADs
Lost A-LADs
Gained B-LADs
Lost B-LADs
log2RPKM (LMNA / Input)
log2RPKM (LMNB1 / Input)
-2.0kb
5'
3'
2.0kb
WT_Rep1
WT_Rep2
MAD_Rep1
MAD_Rep2

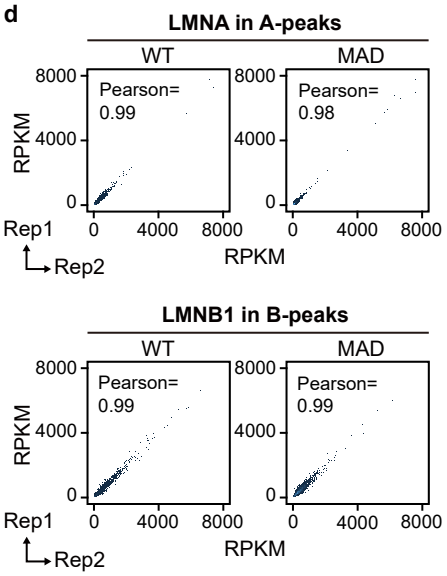
d
LMNA in A-peaks
LMNB1 in B-peaks
WT
MAD
Pearson= 0.99
Pearson= 0.98
RPKM
Rep1
Rep2

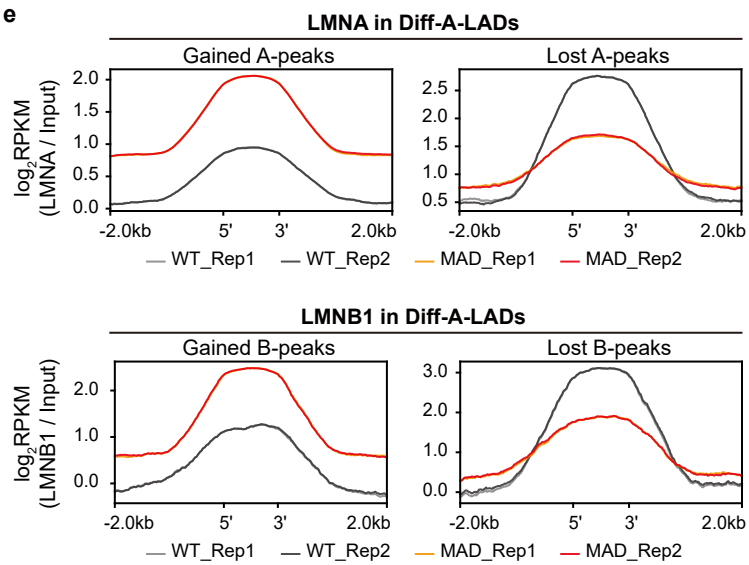
e
LMNA in Diff-A-LADs
LMNB1 in Diff-A-LADs
Gained A-peaks
Lost A-peaks
Gained B-peaks
Lost B-peaks
log2RPKM (LMNA / Input)
log2RPKM (LMNB1 / Input)
-2.0kb
5'
3'
2.0kb
WT_Rep1
WT_Rep2
MAD_Rep1
MAD_Rep2

Supplementary Fig. 18 | Similarity between replicates. a, Scatter plots showing overall signal changes of indicated datasets. For RNA-seq, ATAC-seq and ChIP-seq, x- and y-axis values represented RPKM (reads per kilobase million mapped reads). For ATAC-seq and ChIP-seq of CTCF, H3K27ac, H3K27me3 and H3K9me3, quantifications were performed on the consensus peaks of the two replicates. For ChIP-seq of lamin A/C (LMNA) and lamin B1 (LMNB1), quantifications were performed on 100kb genomic bins. b, Scatter plots showing overall signal similarity between the two independent ChIP-seq for lamin A/C (LMNA) and lamin B1 (LMNB1) LADs. c, Average plots showing the Lamins signals in the differential LADs. Log2RPKM was calculated in 10kb-resolution. d, Scatter plots showing overall signal changes of indicated datasets. x- and y-axis values represented RPKM. Quantification was performed on the consensus A-/B-peaks of two replicates.e, Average plots showing the Lamins signals in the differential Lamin-peaks. Log2RPKM was calculated in 1kb-resolution. All p-values were determined using the two-sided Wilcoxon rank-sum test.

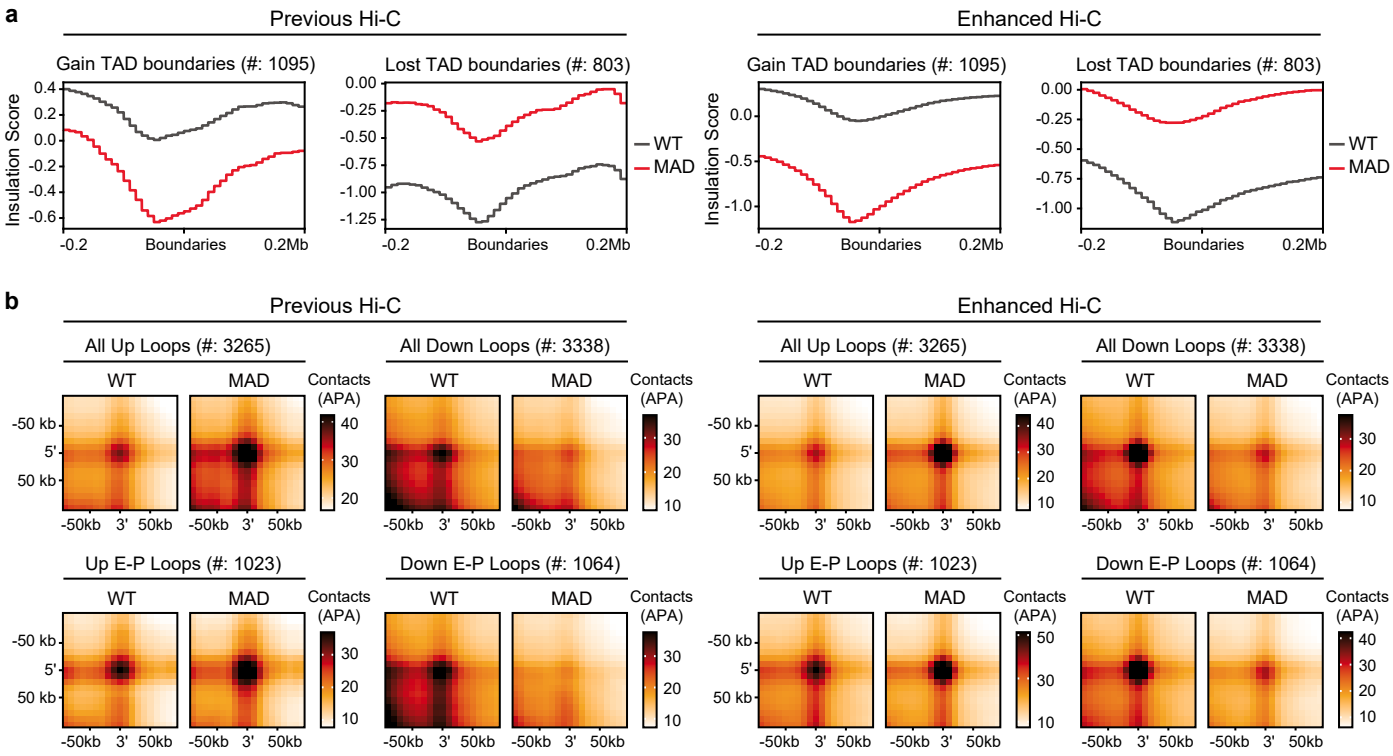
a
Previous Hi-C
Enhanced Hi-C
Gain TAD boundaries (#: 1095)
Lost TAD boundaries (#: 803)
Insulation Score
Boundaries
-0.2
0.2Mb
WT
MAD
b
All Up Loops (#: 3265)
All Down Loops (#: 3338)
Up E-P Loops (#: 1023)
Down E-P Loops (#: 1064)
Contacts (APA)
-50 kb
5'
50 kb
-50kb
3'
50kb

Supplementary Fig. 19 | Validation of differential TADs and loops with enhanced Hi-C data. a, Average plots of insulation scores around differential TAD boundaries. The insulation scores were calculated by GENOVA at 10kb resolution. Lower insulation score represented stronger TAD insulation. b, APA analysis at 10 kb resolution showing the contacts of the indicated interactions in the indicated groups.

NSCs

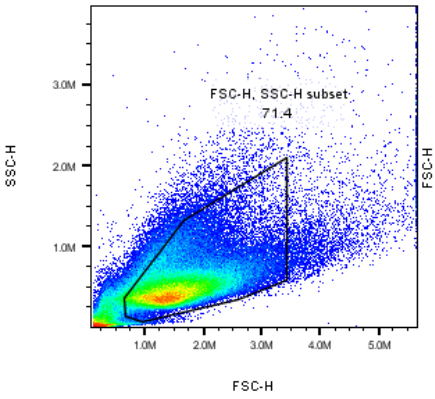

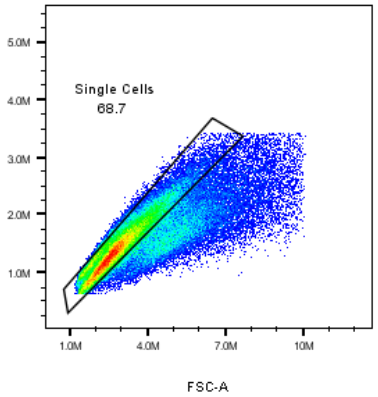

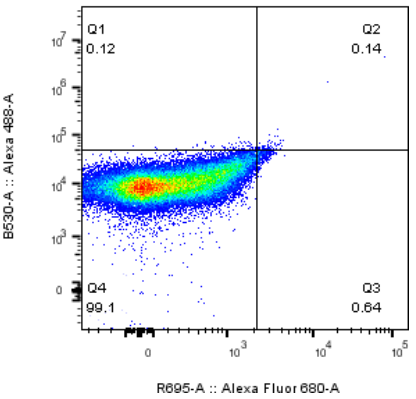

VSMCs

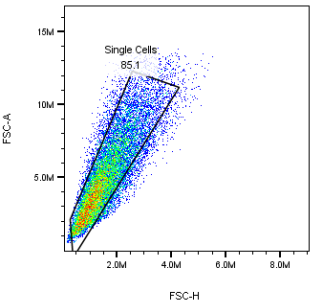

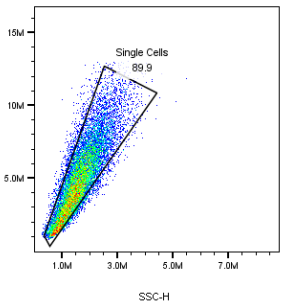

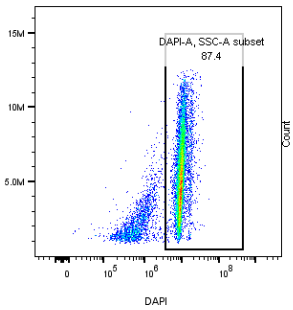

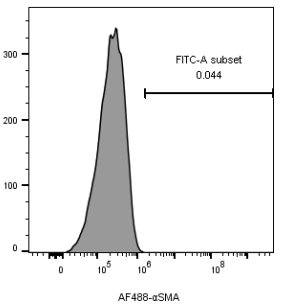

VECs

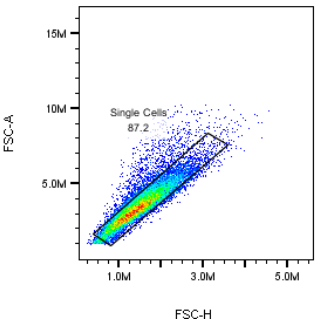

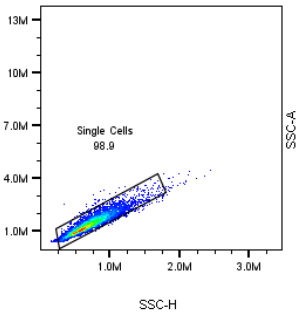

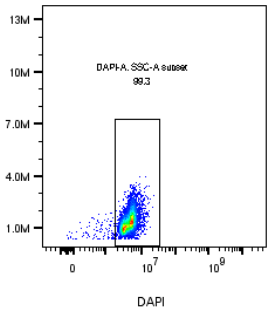

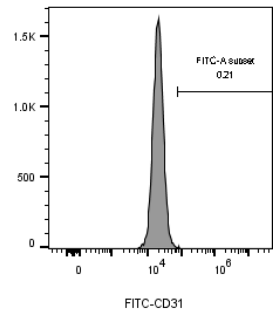

MSCs

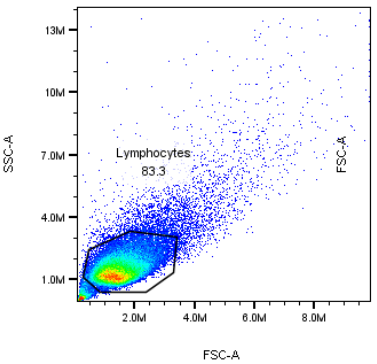

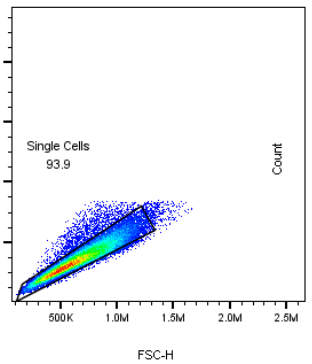

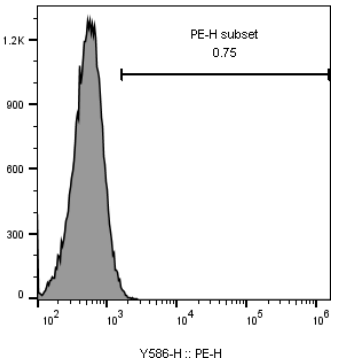

Supplementary Fig. 20| Gating strategy of flow cytometry for NSCs, VSMCs, VECs and MSCs.

Figure 1d, LMNA and β-Actin

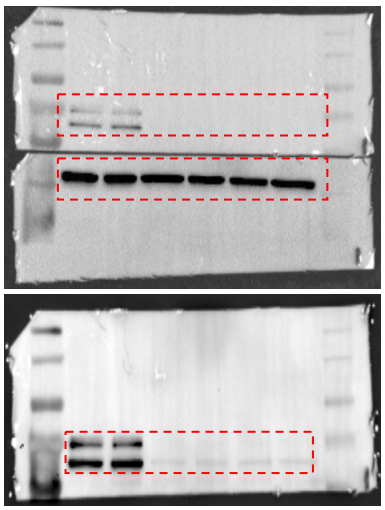

Figure 1d, EMERIN and HP1a

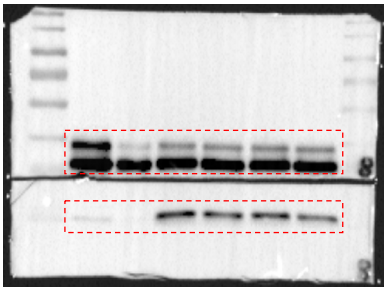

Figure 1d, Ku70 and β-Actin

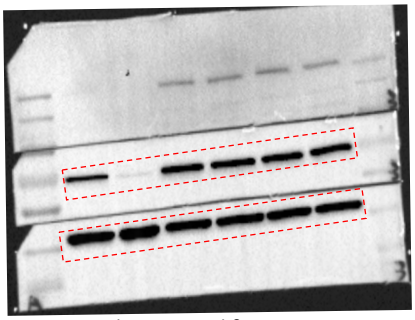

Figure 1d, LAP2

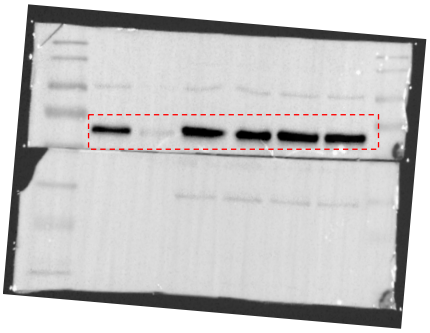

Figure 1d, FOX3A and β-Actin

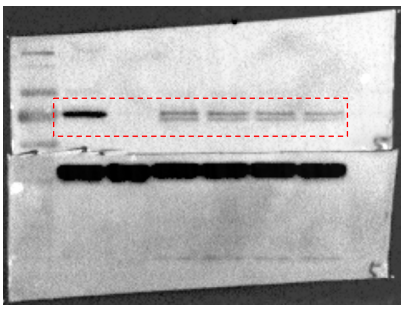

Figure 1d, LMNB1 and β-Actin

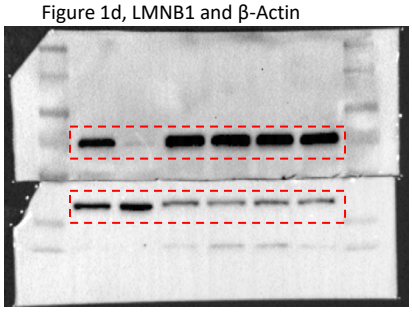

Figure 1d, WRN and β-Actin

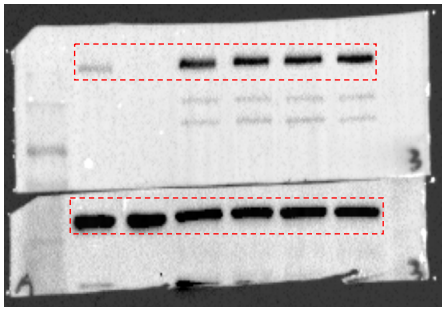

Figure 1d, HADC2 and β-Actin

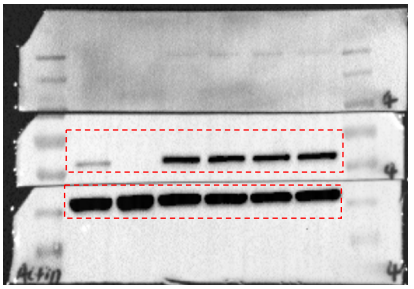

Figure 1d, LMNB2 and β-Actin

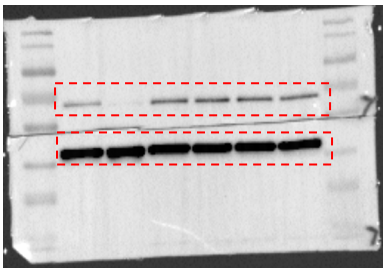

Supplementary Figure 1d, Lamin A/C and β-Actin

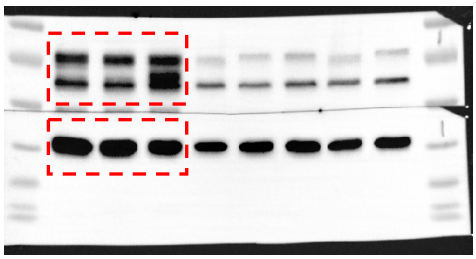

Supplementary Figure 1h, p16,p21 and β-Actin

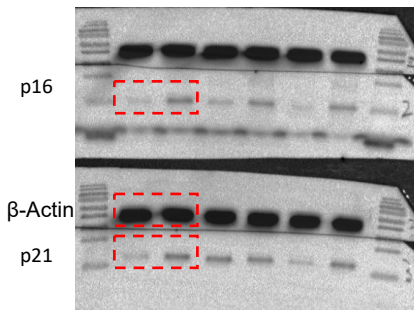

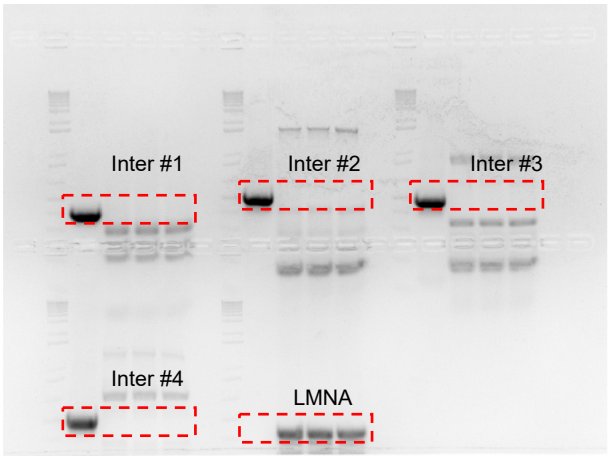

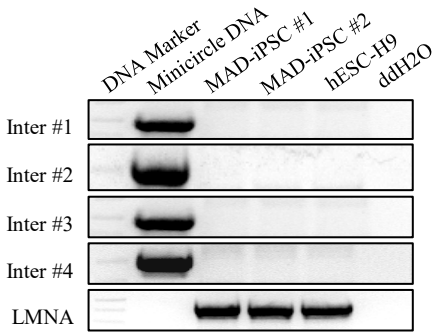

Long-time exposure

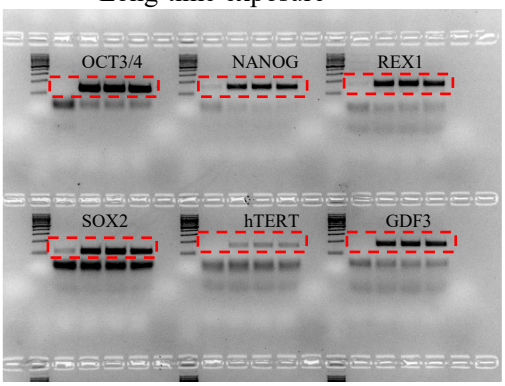

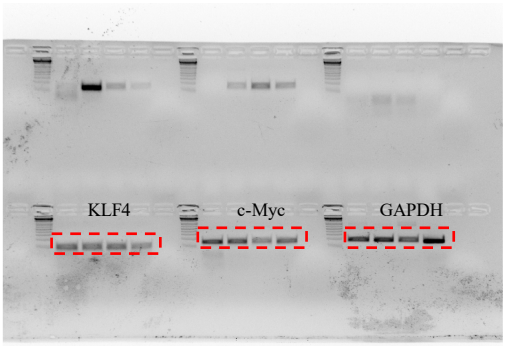

Short-time exposure

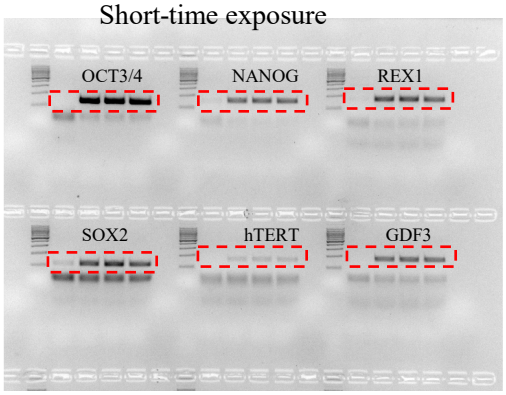

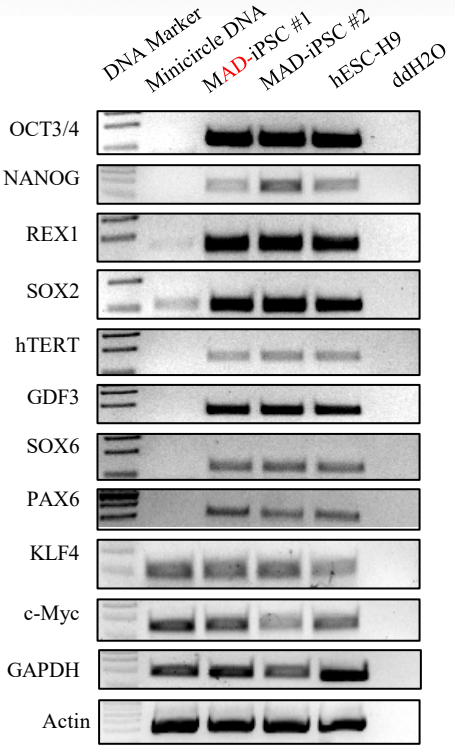

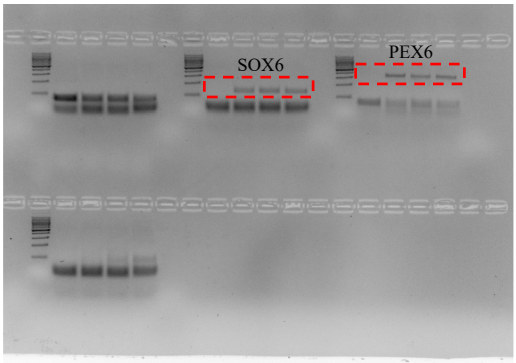

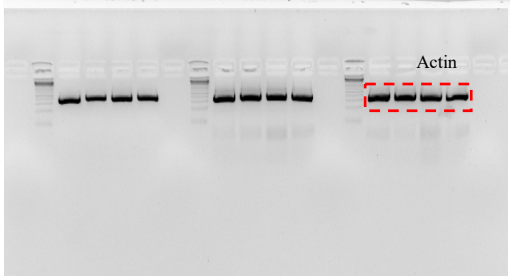

Supplementary Fig. 21| Unprocessed gel for WB and DNA.